A SURVEY ON S-BAND PHASE SHIFTERS

A THESIS SUBMITTED TO
THE GRADUATE SCHOOL OF NATURAL AND APPLIED SCIENCES
OF
MIDDLE EAST TECHNICAL UNIVERSITY

BY
BİLGİN KIZILTAŞ

IN PARTIAL FULLFILLMENT OF THE REQUIREMENTS
FOR
THE DEGREE OF MASTER OF SCIENCE
IN
ELECTRICAL AND ELECTRONICS ENGINEERING

SEPTEMBER 2013

Approval of the thesis:

A SURVEY ON S-BAND PHASE SHIFTERS

submitted by **BİLGİN KIZILTAŞ** in partial fulfillment of the requirements for the degree of **Master of Science in Electrical and Electronics Engineering Department, Middle East Technical University** by,

Prof. Dr. Canan Özgen
Dean, Graduate School of **Natural and Applied Sciences** _____

Prof. Dr. Gönül Turhan Sayan
Head of Department, **Electrical and Electronics Eng.** _____

Prof. Dr. Seyit Sencer Koç
Supervisor, **Electrical and Electronics Eng. Dept., METU** _____

Examining Committee Members:

Prof. Dr. Canan Toker
Electrical and Electronics Eng. Dept., METU _____

Prof. Dr. Seyit Sencer Koç
Electrical and Electronics Eng. Dept., METU _____

Prof. Dr. Şimşek Demir
Electrical and Electronics Eng. Dept., METU _____

Assoc. Prof. Dr. Lale Hayırlıoğlu Alatan
Electrical and Electronics Eng. Dept., METU _____

Bülent Alıcıoğlu, PhD.
REHIS/TTD-MBM, ASELSAN INC. _____

Date: 24.09.2013

I hereby declare that all information in this document has been obtained and presented in accordance with academic rules and ethical conduct. I also declare that, as required by these rules and conduct, I have fully cited and referenced all material and results that are not original to this work.

Name, Last name : Bilgin KIZILTAŞ

Signature :

ABSTRACT

A SURVEY ON S-BAND PHASE SHIFTERS

Kızıltaş, Bilgin
M. Sc. Department of Electrical and Electronics Engineering
Supervisor: Prof. Dr. Seyit Sencer Koç

September 2013, 68 pages

Phase shifters are essential components of beam directing in electronically scanned phased array radar transmitters and receivers that are used in electronic warfare applications for surveillance and self-protection reasons.

In this thesis, initially, fundamentals of phase shifters and various phase shifter topologies are introduced. Afterwards, two-stage all pass filter based phase shifter, eight-section loaded-line phase shifter, aperture coupler based phase shifter and double shunt stub phase shifter circuits are analyzed, designed, fabricated, measured, validated and compared. Investigated circuits are analyzed in MATLAB® and simulations are performed in AWR2009® or HFSS™ design environments. After the design process, circuits are manufactured using PCB technology and measured with a network analyzer. Then, simulation and measurement results are given together for validation. Finally, fabricated circuits are compared.

In this study, a useful resource for S-Band phase shifter design and fabrication is aimed to be exposed meanwhile intending to reveal abilities, limitations, advantages and disadvantages of investigated circuits. Ninety degree phase shift operation throughout the S-Band with maximum of ten degree peak to peak phase error and minimum of ten decibel return loss is aimed for every fabricated circuit in order to compare them in some aspects, namely; electrical performance, size, cost, ease of manufacture and suitability for mass production. Experiments and comments on results are shared throughout the study.

Survey is concluded with revising the experiments and sharing suggestions for future studies.

Keywords: Phased Array Radar, Phase Shifter, Printed Circuit Board, S-Band

ÖZ

S-BANT FAZ KAYDIRICILAR ÜZERİNE BİR ARAŞTIRMA

Kızıltaş, Bilgin
Yüksek Lisans, Elektrik ve Elektronik Mühendisliği Bölümü
Tez Yöneticisi: Prof. Dr. Seyit Sencer Koç

Eylül 2013, 68 sayfa

Faz kaydırıcılar, hedef arama ve kendini koruma amaçlı kullanılan faz dizili alma ve gönderme radarlarında huzme yönlendirmenin temel elemanlarındandır.

Bu tezde, ilk olarak, faz kaydırıcılarla ilgili temel bilgiler verilmiş ve çeşitli faz kaydırıcı tipleri tanıtılmıştır. Sonrasında, iki kademeli tüm geçiren filtre temelli faz kaydırıcı, sekiz bölmeli hat yüklemeli faz kaydırıcı, yüzey etkileşimli kuplör temelli faz kaydırıcı ve ikili şönt hat faz kaydırıcı yapıları analiz edilmiş, tasarlanmış, üretilmiş, ölçülmüş, doğrulanmış ve karşılaştırılmıştır. İncelenen devreler MATLAB® kullanılarak analiz edilmiş ve benzetimler AWR2009® veya HFSS™ tasarım ortamlarında gerçekleştirilmiştir. Tasarım sürecinden sonra, devreler baskı devre teknolojisi kullanılarak üretilmiş ve devre analizörüyle ölçülmüştür. Daha sonra, tasarım ve ölçüm sonuçları bir arada verilerek sonuçlar doğrulanmıştır. Son olarak üretilen devreler karşılaştırılmıştır

Bu çalışmada, incelenen devrelerin yetenekleri, sınırları, avantajları ve dezavantajları açığa çıkarılmaya çalışılırken S-Bant faz kaydırıcı tasarımı ve üretimi hakkında kullanışlı bir kaynak ortaya koymak amaçlanmıştır. Üretilen devreleri elektriksel performans, büyüklük, maliyet, üretim kolaylığı ve seri üretime uygunluk ölçütleri bakımından karşılaştırmak amacıyla her bir incelenen devre için S-Bant boyunca doksan derece faz kayması, tepeden tepeye en fazla on derece faz hatası ve en az on desibel geriye dönüş kaybı hedeflenmiştir. Deneyimler ve sonuçlar üzerine yorumlar çalışma boyunca paylaşılmıştır.

Araştırma, deneyimlerin üzerinden geçilerek ve gelecek çalışmalar için öneriler paylaşılarak sonuçlandırılmıştır.

Anahtar Kelimeler: Faz Dizili Radar, Faz Kaydırıcı, Baskı Devre Kartı, S-Bant

To my beloved family

ACKNOWLEDGEMENTS

I would like to express my most sincere appreciation to my adviser, Prof. Dr. Seyit Sencer Koç, for his invaluable guidance, assistance and patience throughout this study. I would also like to thank Prof. Dr. Canan Toker, Prof. Dr. Şimşek Demir, Assoc. Prof. Dr. Lale Hayrlıoğlu Alatan and PhD. Bülent Alıcıoğlu for attending to my jury and sharing their opinions.

I must send my special thanks to Mr. Kaan Temir, without whose technical support and friendship, it would be definitely far more difficult to accomplish this thesis. I am grateful to Mr. Erdal Saygıner, Mr. Hüseyin Aydın Yahşi, Mr. Mesut Göksu, Mr. Murat Sencer Akyüz, Mr. Şakir Karan, Mr. Sercan Aydoğmuş, Mr. Hüseyin Yalçın, Mr. Gökhan Boyacıoğlu, Mr. Eser Erkek, Mr. Ömer Öçal, Mr. Hayati Tan, Mr. Alper Seren, Mr. Murat Sertkaya, Mr. Onur Şahin and all my teammates at ASELSAN A.Ş. for their helps during the preparation of this thesis.

I am thankful to ASELSAN A.Ş. for their encouraging policy and vision beside technical opportunities and laboratory facilities which were indispensable on the way of completion of this thesis.

I shall declare my gratitude to my friends Kerem Şahin, Engin Sancak, Pınar Beşkesik, Elif Kılıçtek, İslam Tete, Cem Sümengen, Arda Varılsüha, Fırat Erciş, Sercan Sürücü, Hilal Hilye Canbey, Deniz Bulgan and Salih Coşkun for their being helpful and understanding.

I probably cannot pay their support back to my family and Pınar Aka, whose endurance, encouragements and love gave me the strength to fulfill my study.

TABLE OF CONTENTS

CONTENTS

LIST OF TABLES

TABLES

LIST OF FIGURES

FIGURES

LIST OF SYMBOLS

SYMBOLS

AC	: Aperture Coupler
AM/PM	: Amplitude Modulation /Phase Modulation
APF	: All Pass Filter
AWR	: Advanced Wireless Revolution
BPF	: Band Pass Filter
BST	: Barium Strontium Titanate
COTS	: Commercial off-the Shelf
DC	: Direct Current
EM	: Electro-Magnetic
EMC/EMI	: Electro-Magnetic Compatibility / Electro-Magnetic Interference
FET	: Field Effect Transistor
HFSS	: High Frequency Structural Simulator
HMIC	: Hybrid Microwave Integrated Circuit
HPF	: High Pass Filter
IC	: Integrated Circuit
LASER	: Light Amplification by Stimulated Emission of Radiation
LL	: Loaded-Line
LPF	: Low Pass Filter
LTCC	: Low Temperature Co-fired Ceramic
MATLAB	: Matrix Laboratory
MEMS	: Micro Electro Mechanical System
MMIC	: Monolithic Microwave Integrated Circuit
PAR	: Phased Array Radar
PCB	: Printed Circuit Board
PIN	: Positive-Intrinsic-Negative
RADAR	: Radio Detecting and Ranging
RF	: Radio Frequency
RHMM	: Right Hand Metamaterial
RMS	: Root-Mean-Square
S-Band	: 2–4GHz
SMD	: Surface Mount Device
SOLT	: Short-Open-Load-Thru
SPDT	: Single Pole Double Throw
SRF	: Self Resonant Frequency
SS	: Shunt Stub
T/R	: Transmitter /Receiver
TL	: Transmission Line
TTD	: True Time Delay
UWB	: Ultra Wide Band

CHAPTER 1

INTRODUCTION

1.1 Preface

An ideal phase shifter is a two-port device that performs controllable phase shift between its input and output ports without changing the amplitude response. An ideal phase shifter also exhibits a constant phase shift over the design band. However, in practice, a phase shifter represents amplitude and phase errors which should be minimized. Matrix representation of a phase shifter is given in Appendix A.

Phase delay between input and output ports of the reference state of a phase shifter is named as insertion phase. Most basic separation of phase shifters can be done by grouping them as constant and differential phase shifters. Constant phase shifters give a determined amount of phase shift which is the insertion phase of the network. On the other hand, differential phase shifters give the difference between insertion phases of two states; namely reference and difference states. These two states are two different networks and a kind of switching is done between them in order to create the phase shift operation.

As shown in Figure 1-1, an ideal phase shifter shifts the phase of the incoming signal by an amount of its insertion phase without changing its amplitude. Theoretically, voltage at the output port is $V_2 = V_1 e^{-j\Phi}$ when $V_1 e^{-j0}$ is applied to the input port [1].

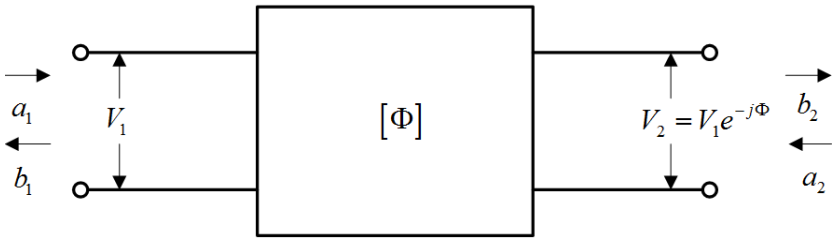

Figure 1-1 General Block Diagram of a Phase Shifter

In broadcasting and communication systems, phase shifters are used in single side band mixers, vector modulators and balanced amplifiers. They are also utilized to reduce phase and frequency errors in phase-locked loops to clean the received signal. With a similar sense to PAR applications, they are used in steering the beam of base stations. Phase shifters are also utilized in feedback networks to lessen the AM/PM distortion of power amplifiers [2]. They are also utilized in high precision measurement and instrumentation systems and industrial applications. Usage of phase shifters in phased array radars is symbolized in Figure 1-2.

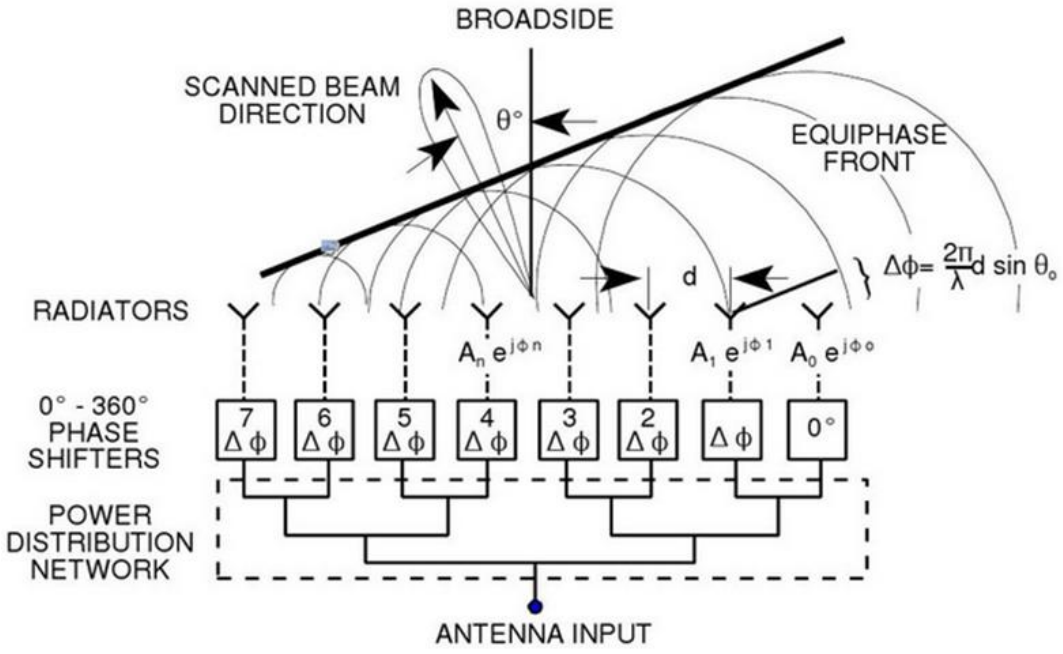

Figure 1-2 Representational Eight-Element Phased Array Antenna System

Studies on phase shifters are generally focused on providing UWB operation with high resolution (in multibit design) and low phase error.

In this study, a useful guide for S-Band phase shifter design and fabrication is aimed to be exposed meanwhile revealing abilities, limitations, advantages and disadvantages of some phase shifter topologies.

1.2 A Brief Review of Previous Works in Phase Shifter Networks

First examples of phase shifters come to existence in 1940's. Rotary vane adjustable phase shifter is introduced by Fox in 1947 [3]. In 1950's no matter fixed or variable, most phase shifters were mechanical.

In 1957, Reggia and Spencer proposed an analog phase shifter. This device is a primitive electronically variable phase shifter and has a magnetized ferrite core at the center of a rectangular waveguide [4].

1958 is a milestone in phase shifter history. With the use of coupled transmission lines, B. M. Schiffman realized a 90º differential phase shifter that is matched over a broad band [5]. Schiffman topology is based on two distant transmission lines, one of which is parallel-coupled to be dispersive. By the proper selection of dimensions of transmission lines, differential phase between the arms can be set to 90° over a considerably broad band.

General synthesis process of the conventional Schiffman phase shifter is explained in [6]. Stripline design is preferable to microstrip design because homogeneous medium that supports TEM wave allows even and odd modes to propagate with the identical phase velocities through the coupled lines. However, necessity of narrow gap between the coupled lines in order to achieve tight coupling is the main problem of Schiffman phase shifter. Nowadays, this problem may be reduced to some level using thin film technology instead of PCB technology.

Even and odd mode velocities are closened by using cascaded coupled lines in [7]. Manufacturing difficulty due to the need for narrow aperture between the coupled lines of this circuit is lessened in a similar configuration that is based on cascaded unequally coupled parallel transmission line sections [8].

With an improvement to Schiffman phase shifter, wide band edge coupling causing a smooth phase response with small phase fluctuations and a good VSWR over more than 90% bandwidth is achieved by multi-sectioning the parallel connected stages [9]. However, small gap between lines and necessity of high impedance lines cause fabrication difficulties. Another modified Schiffman topology is presented in [10]. Capacitor effect is generated by a rectangular conductor that is located below the coupled lines. 180º phase shifter with 5º phase imbalance within 1.5GHz-3.1GHz band is fabricated.

In [11] and [12], switching is performed between a part that consists of $\lambda/2$ wavelength coupled transmission lines and $\lambda/8$ shunted stubs and a transmission line part. Broadband 180º bit phase shifters operating between 1.5-4.5GHz with 12dB return loss and 10º phase fluctuation are designed and manufactured.

In [13], compact 45º dumb-bell shaped phase shifter that consists of open circuit and short circuit multisection stubs is achieved with 6.5º phase imbalance over 2-6GHz band.

An UWB phase shifter operating over the 4.5-18GHz range is explained in [14]. Full coverage of 360º is achieved by cascading a digital 180º with an analog 180º section.

In digital phase shifter section, FET switching is applied between π-networks that behave as band-pass filters. Experimental results are as follows: 177±7º phase response over 2-17GHz band, insertion loss of 2.3±0.8dB over 4-17.5GHz band, worst case amplitude imbalance of 1.2dB over 2-17.5GHz band, better than 10dB return loss over 6-18GHz band and minimum of 8dB return loss over 4-18GHz.

In analog phase shifter section, varactor diodes in series with a small bond wire inductance are employed as terminations of a conventional 3dB four finger interdigital coupler. Voltage is biased via chip resistors and DC blocking capacitors that are utilized for the isolation of RF plane from the DC plane. Voltage bias between +0.5V to -30V provides a minimum of 160º phase coverage within 4.5-18GHz band. Insertion loss is 4.5dB within 4.5GHz-18GHz band in the worst case.

In order to improve the performance of the circuit, it is advised to cascade two 90º analog sections operating at their best regions instead of one 180º section. Another suggestion is to employ phase calibration by utilizing a smart silicon driver that operates in accordance with a look up table.

A 5-20GHz 90º MMIC reflection type phase shifter that is operating either in digital or analog mode is introduced in [15]. In the analog operation, any phase shift value from 0º to 90º can be obtained by controlling the FET's gate bias voltage. Phase imbalance is less than 5º in the manufactured circuit.

Amin M. Abbosh proposed an UWB compact planar phase shifter in [16]. This technique benefits from the constant broadside coupling that is created between top and bottom elliptical microstrip patches via an elliptical slot located in the mid layer. Exterior part of the slot of the mid-layer forms the ground plane. 30º and 45º phase shifters operating between 3.1-10.6GHz are realized with the proposed structure. Maximum of 6º phase error, better than 10dB return loss and less than 1dB insertion loss is achieved within the design band.

Termination networks that can be used in reflection type phase shifters are introduced in [17]. A significant outcome of this study is that the bandwidth of the phase shifter is limited by the body network (e.g. a 3dB coupler or a circulator) rather than the termination network.

In [18], a successful technique is offered in order to have wideband operation and larger phase shift values by eliminating the resonances causing notches in the amplitude response and large errors in the phase response.

It is exposed that transmission type phase shifters that use PIN diodes as control elements are convenient for L-Band and S-Band PAR implementations [19].

Miniature size phase shifters operating at L-Band and S-Band are designed applying HMIC technology to PIN diode based digitally controlled phase shifter networks in [20]. Additionally, feasibility of applying microstrip technique on alumina ceramic for phase sensitive circuitry is demonstrated.

The study on all pass LC filter circuits in [21] pointed out that all-pass circuits of 2^{nd} order can be realized without being obstructed by mutual inductance for $Q<1$ case. By the proposed circuit, 1^{st} order all-pass circuits became applicable for the high frequency area because mutual inductances between coils no longer obligatorily have ideal unity coupling coefficient.

In [22], an ultra-compact 5 bit MMIC phase shifter is designed using lumped element all pass filter circuitry. Transition frequency of an all pass filter network has to be larger than the operating frequency for a compact design.

All pass filter networks are cascaded in series using thin film BST varactors to design a compact, low loss, low cost analog 360º MMIC phase shifter in [23]. All pass filter networks are cascaded in a manner that center frequencies of each section are staggeredly placed. This technique provided broad-band constant phase shift value with a small amplitude imbalance. Additionally, tuning ability of thin film BST varactors played important role on achieving low loss, low cost design.

D. Adler and R. Popovich reported that broadband phase shifting can be obtained by switching between all pass filter networks [24]. Bandwidth can be increased by cascading all pass sections with staggered center frequencies. In this work p, q and Ω parameters are introduced for calculation of COTS component values to have desired electrical performance over the design band. However inductor and capacitor values decrease significantly as the operating frequency or number of cascaded sections or phase resolution increases. Bandwidth cannot be increased infinitely by increasing the number of cascaded stages due to the non-distributive nature of the components. Octave-band four bit phase shifter with less than ±6º phase error is successfully manufactured.

MEMS switching appears to be a solution for high insertion loss problem of PIN diode or FET switching that is especially encountered in high frequency applications. However, switching speed of MEMS is quite bad due to its mechanical characteristics [1], [25].

Digitally controlled MEMS switching reflection type phase shifter design is explained in [26]. An UWB MEMS phase shifter covering 0º to 90º over 5-17GHz band with 3.5dB average insertion loss and ±1.80º RMS phase error is fabricated and measured.

11.25º, 22.5º, and 45º phase shifters operating over 10.7-12.75GHz band are designed and manufactured in [27]. These structures include shunted MEMS switches beside open and short ended stubs.

MMIC technology is being applied on manufacturing MMIC phase shifters since 1980's. In [28] MMIC and HMIC technologies are compared amongst them. MMIC phase shifters operating within 2-6GHz and 4.5-18GHz bands with less than 15º and 20º phase imbalance respectively, are manufactured in [29]. 180º, 90º, 45º and 22.5º/11.25º divisions are designed independently and then combined to form a 5 bit phase shifter. The challenge in this design is to keep both phase and amplitude variations as small as possible despite the impedance variation caused by the FET switching of reflective terminations. However, proposed phase shifter seems to lack in decision of equal division of the phase coverage. In other words, 33.75 degree phase shifting circuit should be added to 22.5/11.25 degree section in order to cover the 360 degree with equal steps. Nevertheless, such a design may have been done on purpose.

UWB hybrid coupled phase shifter that consists of a Lange coupler, radial stubs, switching diodes, bias networks and capacitive reflective loads is designed by Kwon, Lim, and Kang in [30]. Capacitive reflective loads are placed at the direct and coupled ports while input and isolated ports are used as input and output ports. PIN diodes are used as switching elements between the identical termination circuits and wideband RF signals are grounded by radial stubs. Frequency dependency of coupling coefficient of the unfolded Lange coupler should be taken into account in the design process. Designed phase shifters exhibited 4.4º, 4.4º, 7.2º and 11º phase errors for 11.25º, 22.5º, 45º and 90º phase shifter circuits respectively.

6-18GHz 5 bit MMIC phase shifter consisting of a 3dB Lange coupler, FET switches and reflective terminations is demonstrated in [31]. Switching is done between MMIC reflective termination circuits consisting of two-stage series and parallel resonant circuits. Bandwidth is limited by the Lange coupler part as termination part has 183±3º phase imbalance over 0.5-30GHz band while the performance of whole structure is 187±7º over 0.5-20GHz.

7-11 GHz MMIC 6-bit phase shifter is designed in [32]. PIN diodes are utilized for switching between high-pass and low-pass filter sections in order to create the desired phase shift value. 180º, 90º, 45º, 22.5º, 11.25º and 5.625º bits are designed separately and cascaded to have 360º phase coverage. A MESFET switched high-pass and low-pass filters and radial stubs are utilized in MMIC 1-22GHz 90º phase shifter design [33].

Idea of designing a metamaterial phase shifter could not wait much after the developments in this popular subject. Lee et. al. designed a quadrature coupler based phase shifter utilizing Wilkinson power dividers, delay lines and crossovers [34]. 90º±5º phase performance and 1.2dB amplitude imbalance between the output ports of quadrature hybrid is achieved over an octave band.

Kholodnyak et. al. decided to switch between positive and negative dispersion transmission lines in [35]. Idea seems to be logical since artificial transmission lines behave like filters. Therefore, the structure can be considered as a switched filter phase shifter. 2.0-3.6GHz digital phase shifter with 180±7º phase performance and 11dB return loss at worst case is designed and fabricated.

Yongzhuo et. al. added an improvement to Schiffman phase shifter in [36]. Coupled line part of conventional Schiffman phase shifter is replaced with a novel RHMM transmission line. Existence of non-zero phase constants at DC in RHMM transmission line unlike the normal transmission line is the reason why this idea works.

FET switching MMIC high-pass low-pass topology is investigated in detail by Ayaslı et. al.[37], [38]. 90º and 180º phase bits operating between 2-8GHz and 8-12GHz respectively are realized on GaAs substrate.

CHAPTER 2

PHASE SHIFTER REQUIREMENTS, CLASSIFICATION AND TOPOLOGIES

2.1 Phase Shifter Performance Requirements

In general, electrical, mechanical, industrial and environmental performance parameters can be defined for phase shifters. Numerical limits to the element requirements come from module requirements that are extracted from system requirements. However, it is not possible to satisfy all requirements with any of the phase shifter types [39]. The hierarchy of design parameters is defined by the application area. Trade-offs between parameters should be done without sacrificing from minimum acceptable performance limits. It would be wise for a designer to make the topology and technology selection that is more likely to meet the specified requirements. In simulation step, real effects should be involved as much as possible by doing EM simulations, embedding S-parameter files, etc. A realistic tolerance should be taken into account and worst case analysis should be done before production.

2.1.1 Operating Frequency Band and Return Loss

Operating frequency band is the initial design parameter that defines lower and upper frequencies of operation, hence the bandwidth. All other performance criterion should be satisfied within the operating frequency band.

Return loss is a type of loss that is caused by the impedance mismatches at input and output ports and discontinuities at the RF strip. Measurement of return loss is done according to the proportion of transmitted and reflected powers. Bad input return loss causes some amount of applied power to be reflected into the source. Bad output return loss causes some amount of applied power to be reflected into the circuit. Deficiency of both input and output return loss result in amplitude and phase distortions in the system response. In order to have a good cascaded system performance, return loss should be kept as good as possible both individually and concomitantly. Formulas of input and output return losses of a phase shifter are given as

$$Input\ Return\ Loss: IRL(dB) = -20\,log_{10}|S_{11}| \tag{2.1}$$

$$Output\ Return\ Loss: ORL(dB) = -20\,log_{10}|S_{22}| \tag{2.2}$$

Using attenuator at the input port increases input return loss and using attenuator at the output port increases output return loss. However, some performance parameters such as noise figure, gain, etc. should be considered before such decision.

2.1.2 Differential Phase Shift and Phase Shift Error

Insertion phase is the phase difference between the input and output ports of any device. The formula for insertion phase is given as

$$Insertion\ Phase: \emptyset_{21} = -\tan^{-1}\left[\frac{Im\{S_{21}\}}{Re\{S_{21}\}}\right] \quad (2.3)$$

Differential phase shift is the phase difference between insertion phases of reference and difference paths. Differential phase shift is defined as

$$Differential\ Phase\ Shift: \Delta\emptyset_{21} = \emptyset_{21}^{(1)} - \emptyset_{21}^{(2)} \quad (2.4)$$

Phase error may be caused by temperature variation, input power variation, etc. Most popular error definitions are peak to peak phase error and RMS phase error definitions. Even though both error values should be kept as small as possible, RMS phase error can be tricky. For example, a 90º phase shifter with 20º peak to peak error in a short duration in the band may make the phase shifter unusable. However, it is possible that the same circuit has a small RMS phase error value. Nevertheless, before the designing a phase shifter, having both peak-to-peak error and RMS error limitations may be a better idea.

Phase resolution cannot be less than phase error. In a digital phase shifter, it is not acceptable for two different states to intersect in the frequency band. Phase errors may cause undesired effects in PAR beam pattern and can be minimized to some level by holding a calibration table. In order to have flat phase response, phase and amplitude fluctuations should be kept as small as possible.

2.1.3 Insertion Loss and Amplitude Imbalance

Insertion loss is measure of transmission losses that are created by component loss, impedance mismatches and conductor losses, etc. Signal attenuation caused by insertion loss causes power dissipation and may bring up amplification requirement, hence heat sinking problems. What is more, due to the fact that phase shifters are used as very beginning elements of receivers, insertion loss should be kept as small as possible in order not to decrease the signal-to-noise ratio of the system. Formula of the insertion loss of a phase shifter is given by the following formula.

$$Insertion\ Loss: IL(dB) = -20\,log_{10}|S_{21}| \quad (2.5)$$

In digital phase shifters, increasing the number of bits means increasing the number of cascaded stages and switching elements, hence the insertion loss. Moreover, widening the operating band of the device will probably increase the insertion loss.

Amplitude imbalance is insertion loss difference between reference and difference paths of a phase shifter and it is source of phase imbalance.

2.1.4 Phase Sensitivity and Phase Resolution

A highly sensitive analog phase shifter can scan all the phase coverage with small phase shift steps. Since phase shift is provided by capacitance variation that is created by the applied voltage, phase sensitivity is determined by the success of voltage leveling circuitry in analog phase shifters.

In digital phase shifters, phase resolution of a phase shifter is the minimum phase shift angle that can be performed by a phase shifter under the condition that phase coverage is divided equally. Phase resolution of a digital phase shifter is determined by phase coverage and number of bits. Phase resolution can be stated as

$$Phase\ Resolution: \Delta\emptyset = PC/2^n \tag{2.6}$$

where

PC: Phase coverage

n: Number of cascaded stages under the condition that each stage has two states

$$\text{Total Phase Shift: } \emptyset = \Delta\emptyset\times\text{"bit\_0"} + 2\Delta\emptyset\times\text{"bit\_1"} + \cdots + \left(\frac{\text{PC}}{2}\right)\times\text{"bit\_n"} \tag{2.7}$$

Although, in theory, it is possible to increase the phase resolution infinitely, it is meaningless to design a phase shifter that has more phase error than its phase resolution. In phased array applications, having high phase resolution is important to have good beam steering resolution and small side-lobe levels. On the other hand, increasing the phase resolution may increase the insertion loss, cost, size and complexity of the circuit.

2.1.5 Power Handling Capacity and Power Consumption

Phase shifters are generally located at the beginning section of receivers or at the ending section of transmitters. Unquestionably, transmitter part is more problematic due to the high power handling requirements. In passive digital phase shifters, power consumption is caused by driver circuit. Insertion loss decreases the energy efficiency. Power efficiency and consumption are more important parameters in active phase shifters where a discrete amplifier is employed with a phase shifter. Wherever they are located, phase shifters should be designed to handle the required peak power and continuous operating power; and it is preferable to design energy efficient and low power consuming phase shifters.

2.1.6 Driver Circuit and Tuning Time

Driver circuits are necessary to give the required control voltages to the control inputs of phase shifters. Appropriate biasing should be applied while avoiding complexity. Power planning of driver circuit is important in order to prevent heat sink problems in the circuit.

Tuning time of a phase shifter is the amount of time that is elapsed between applying either an RF signal to the RF input port or control signal to the control inputs and getting the relevant expected signal settled at the output port.

Tuning time is an important design parameter as it directly affects the speed of target scanning. Type of the phase shifter is very important for a good tuning time e.g. electronical phase shifters are much faster than mechanical phase shifters. Additionally, hysteresis characteristic of ferrite phase shifters provide them an advantage to respond quickly to applied changes.

2.1.7 Compactness, Integrability, Cost and Complexity

A compact phase shifter has small size and weight. Integrability definition is related to shape and packaging. Modern PARs may consist of thousands of elements. Furthermore, in some applications like expandable jammers, there is little room for every RF component. Therefore, like every component, phase shifters should be designed to be compact and integrable.

Cost is a design parameter that may contain many components. Labor cost and material cost are initial costs whereas power consumption and maintenance costs are future costs. Cost minimizing topology and technology selection should be done without sacrificing from other requirements. Cost reduction is very important in large PAR systems. It is very important for any device to be as simple as possible; otherwise generally, circuit gets harder to be manufactured and more expensive.

2.1.8 Reproducibility and Maintainability

Reproducibility is a component of suitability for mass production. A reproducible design is repeatable in an acceptable tolerance level. Maintainability covers many aspects. Reparability is possibility of intervening to problematic part of the circuit without discarding the whole circuit. Designing the circuit open to future developments is modifiability. Also, having higher stability, robustness, disturbance rejection, mean time between failure value and lifetime makes a circuit more maintainable. Contemporary PARs may contain thousands of phase shifters to be manufactured and maintained and that makes all these definitions very important. Technology and topology selection are very important as they affect reproducibility and maintainability of the circuit.

2.1.9 Environmental Requirements and Packaging

Mechanical stress and thermal variation may affect other system requirements. There are many environmental requirements mentioned in military standards. For a specific system, indispensable environmental requirements are defined and they should be obeyed. Packaging defines housing of components. Casing is done according to environmental requirements, mounting needs and EMI/EMC considerations.

2.2 Classification of Phase Shifters

It is reasonable to classify phase shifters in some aspects. Because, once the class properties are understood, it will be easier to choose a proper and adequate topology for a specific problem. A phase shifter may be analog or digital according to type of control operation; mechanical or electronical according to tuning mechanism; fixed or adjustable according to tunability; non-reciprocal or reciprocal according to directionality; PIN diode or FET controlled according to switching type; IC or Ferrite according to production technology; transmission type or reflection type according to circuit configuration. All these topics are mentioned in detail in this section.

2.2.1 True Time Delay and Phase Shifter

Before stepping into classification of phase shifters, nuance between phase shifter and true time delay should be emphasized [40]. This separation of delay devices is made according to design requirements.

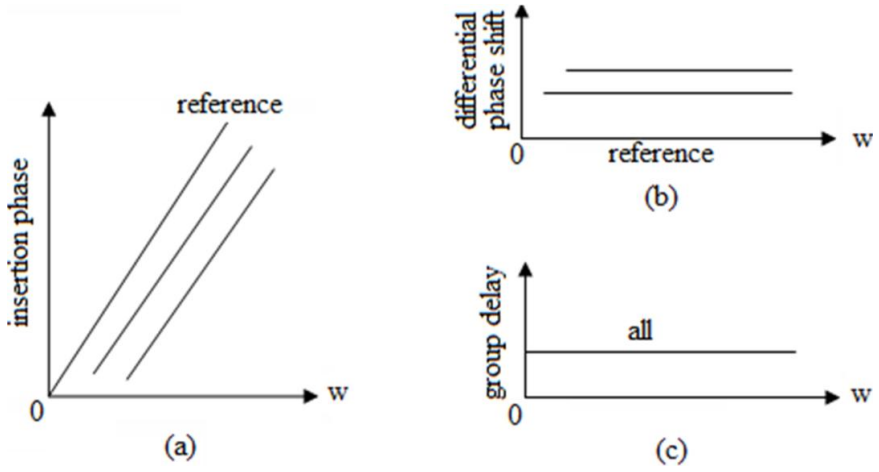

Figure 2-1 Frequency Characteristics of a Phase Shifter
(a) insertion phase, (b) differential phase shift and (c) group delay

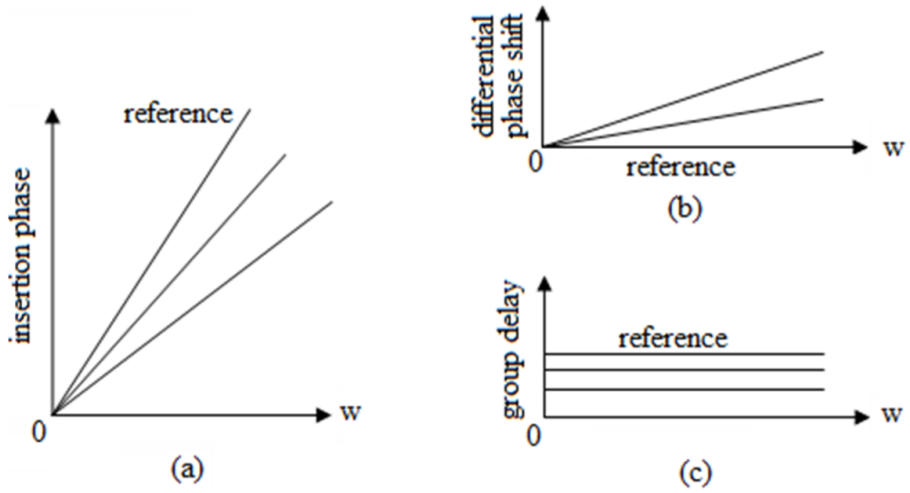

Figure 2-2 Frequency Characteristics of a True Time Delay
(a) insertion phase, (b) differential phase shift and (c) group delay

As it is seen in Figures 2-1 and 2-2, there are certain differences between a true time delay and a phase shifter.

With changing values of insertion phase, true time delay structures give a linearly varying phase shift value with respect to frequency while phase shifters are expected to give a constant phase shift value over the operating frequency range.

For a decisive target tracking and application of electronic counter measure techniques, angle resolution should be as high as possible. In order to have a better angle resolution, short pulses in time domain, in other words, wide bandwidth signals in frequency domain should be processed. In applications where instantaneous bandwidth is high, if received signal's time difference between distant array elements is tried to be compensated with phase shifters instead of time delay devices, beam-squinting effects will spoil the beam directivity and pattern [41].

In some applications, both true time delays and phase shifters are utilized to benefit from advantages of both circuits.

2.2.2 Analog Phase Shifters and Digital Phase Shifters

Digital and analog phase shifters are separated according to type of control operation. Analog phase shifters utilize voltage leveling circuitry. Digital phase shifters operate according to their control inputs. As it is seen in Figures 2-3 and 2-4, digital phase shifters may house a number of cascaded stages that are generally tied with a MMIC, MEMS, PIN or FET switch [41].

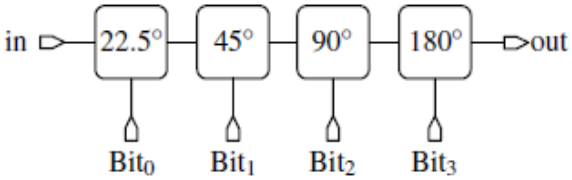

Figure 2-3 Four Bit All Pass Filter Based Phase Shifter Structure

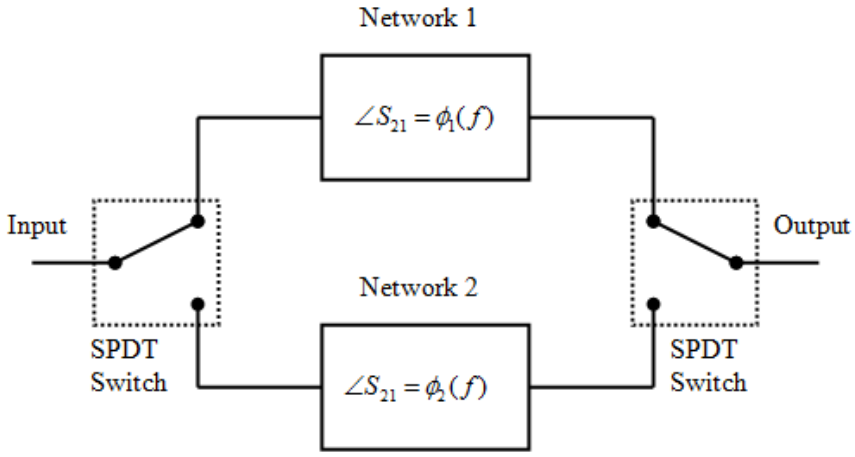

Figure 2-4 Single Bit of an All Pass Filter Based Phase Shifter Structure

Analog phase shifters are expected to have higher operation speed. However, voltage leveling circuitry of an analog phase shifter generally utilizes a digital to analog conversion that wipes some of this advantage out. Analog phase shifters have less insertion loss none the less well pinched-off digital phase shifters offer more stable operation. Being more compact and compatible with computer interfaces, digital phase shifters are more preferable in PAR applications.

Analog phase shifters offer continuous operation; in contrast, digital phase shifters operates discretely. In the design given in [42], coarse tuning is done by digital part of the hybrid structure whereas fine tuning is done by the analog part.

2.2.3 Mechanical Phase Shifters and Electronical Phase Shifters

Phase shifters can be classified according to their tuning mechanism as mechanical and electronical phase shifters. Mechanical phase shifters are more likely to operate in analog nature and they tend to be reciprocal devices. They may be constructed in transmission line or waveguide structures.

Operation of a mechanical phase shifter is generally exampled with a rotating knob that changes the length of a transmission line or rotation-displacement of a dielectric slab inside a waveguide. Mechanical phase shifters are though, easy to fabricate, cheap and suitable for high power applications. However, they are not preferable in PAR applications due to the volume and weight requirements of PARs. Additionally, electronical phase shifters' enormous superiority in switching speed and capability of inertialess scanning makes them indispensable in PAR applications [1].

2.2.4 Fixed Phase Shifters and Adjustable Phase Shifters

Another discrimination of phase shifters is made according to their tunability. Tunability is directly related to the application area. Fixed phase shifters are utilized in Butler matrices and monopulse converters whereas adjustable phase shifters are indispensable elements of electronically scanned PARs [28]. Although an adjustable phase shifter can be used as a fixed one, it is not logical to use them in applications where it is satisfactory to use fixed phase shifters due to cost and circuit complexity matters. Phase shift value of a tunable phase shifter is adjusted by a control interface while fixed phase shifters are designed to give the constant necessary phase shift value [1].

2.2.5 Nonreciprocal Phase Shifters and Reciprocal Phase Shifters

In practice, reciprocal phase shifters can be used bidirectionally whereas non-reciprocal phase shifters can be used in only one direction. Reciprocity property is more meaningful in T/R modules. Using a reciprocal phase shifter on common stripe of a T/R module may reduce cost and weight of the system.

2.2.6 FET Switching and PIN Diode Switching

It is possible to categorize phase shifters according to their switching mechanism. There are numerous switching types. In analog type MIC configurations, varactor diodes are used. In this type, reactance is controlled via a tunable capacitor by applying negative bias voltage. MEMS switching is used in RF MEMS phase shifters. PIN diode switching is preferred in HMIC configurations whereas FET switching is preferred in MMIC configurations. Since PIN diode and FET switching are most commonly used types and relying on the fact they are more suitable for the circuits implemented in this thesis, detailed comparison will be done between this two switching types.

PIN diode switches exhibit low impedance under forward bias, thus operates in on-state. Under reverse bias, high impedance is seen by the signal, so the diode operates in off-state.

In FET switching, source to drain current flow is controlled by gate bias voltage. Under a sufficiently large negative voltage biasing condition, high impedance causes off-state operation. On-state is provided via creating low impedance by applying zero gate bias voltage.

PIN diodes have slightly lower insertion loss than FET switches and they are less susceptible to electro-static discharge.

FET switches can work at DC while PIN diode switches cannot. On the other hand, PIN diode switches may operate at higher frequencies.

PIN diodes are two-terminal devices, whereas FETs are three-terminal devices. The gate terminal of a FET is decoupled from the source and drain. Therefore, in FET switching, there is no need to isolate bias signals from RF signals via a bias tee as in PIN diode switching. Hence, driver circuit of a PIN diode switch is more complex than a FET switch. Moreover, quarter-wave capacitive stubs that are generally involved in biasing network of PIN diodes limit the usable bandwidth of the whole circuit to around one octave. Also, DC blocking capacitors are not needed in the FET design.

FETs solely need a voltage signal for switching, in place for a DC current. That means FETs have zero DC power consumption whereas around 10mW is required to turn on a PIN diode. In a PAR system of 100.000 elements, this slight difference brings extra power consumption of 1kW.

2.2.7 Ferrite Technology and Integrated Circuit Technology

Ferrite phase shifters are generally implemented in wave guides although they may be realized in microstrip form. They are low loss devices that are able to handle high power levels. However they are too large and they have a long switching time to be used in PAR applications. They have complex and expensive design procedure and less reliability than IC phase shifters as permeability of the ferrite material fluctuates significantly according to temperature variations and mechanical stresses.

Twin-toroid phase shifters and Faraday rotation phase shifters are some examples for ferrite phase shifters. On the other hand, HMIC, MMIC, MEMS and BST phase shifters are well-known IC phase shifter types.

IC phase shifters have almost controversial properties with ferrite phase shifters. They are compact and they offer higher switching speed than ferrite phase shifters. [41].These two properties are invaluable in today's PAR systems which may include thousands of array elements and should meet the fast scanning requirements. Once the proper tuning is done, IC phase shifters are cheaper than ferrite phase shifters due to their convenience to mass production. Moreover, IC phase shifters are less susceptible to mechanical stresses and temperature variations; on the other hand they are prone to suffer from variations in either analog or digital control voltages in a bad design.

2.2.7.a MMIC Technology and HMIC Technology

It is logical to handle MMIC and HMIC technologies together in comparison to better understand their properties.

In HMIC technology, design is realized on a PCB that has a certain dielectric constant. As the name suggests, chip diodes or transistors are used together with microwave lines and other elements on the appropriate PCB. In MMIC technology, all the active and passive devices and other necessary functions are built into the same chip [43].

HMIC technology provides easiness in failure diagnosis, debugging, tuning and trimming in the fabricated design. It would not be wrong to agree on the impossibility of modifying the manufactured design in IC technology. On the other hand, repeatability and reliability of MMIC phase shifters is better than HMIC phase shifters. Eventually, once the proper tuning is done and the satisfactory repeatability is achieved in both technologies, a significant reduction in unit cost can be provided by mass production.

MMIC technology offers more compact circuitry than HMIC technology as everything necessary is implemented in the same chip and there is no soldering and bonding between circuit components.

HMIC phase shifters can handle more power than MMIC phase shifters. However, MMIC phase shifters may operate at higher frequencies and may have broader bandwidth due to having less parasitic effects.

2.2.7.b RF MEMS Technology and BST Technology

RF MEMS and BST are popular technologies of recent years and they keep on growing rapidly.

MEMS technology takes its name from assembling mechanical and electronical elements together on the same substrate via micro-fabrication technology. MEMS production process has fewer steps than MMIC production and it offers low-loss, low-cost systems with a good control over capacitance variation. MEMS switches may operate at very high frequencies. Low drive power level requirement, high isolation, compactness and simple circuitry are other good features of MEMS to use them in PAR systems. However, long switching time, low power handling capacity, bad reliability caused by metal failure, dielectric inconsistency and short lifetime are some drawbacks that must be solved in the way of their usage in PAR systems.

BST is a sort of ferroelectric substance whose dielectric constant changes with the amount of applied electric field. Therefore, capacitance per unit length of a transmission line, hence the phase velocity is controlled by the applied electric field. Varactor diodes that are utilized to control analog phase shifters may be designed with the same idea [2].

2.3 Main Phase Shifter Topologies

Differential phase shifters may be separated as transmission type circuits and reflection type circuits upon their circuit configuration. Although many categorization types can be used, classification in Figure 2-5 is decided to be more convenient for the study in this thesis.

Transmission type phase shifters benefit from difference between transmission characteristics of reference and difference paths. Switched-line phase shifters, loaded-line phase shifters and switched-network phase shifters belong to transmission type phase shifter category.

Reflection type phase shifters derive phase difference from difference between reflection characteristics of distinct terminations with same body network. Circulator based and hybrid coupler based phase shifters belong to reflection type phase shifter category.

In this thesis, some topologies that belong to this classification will be analyzed, designed, fabricated validated and compared.

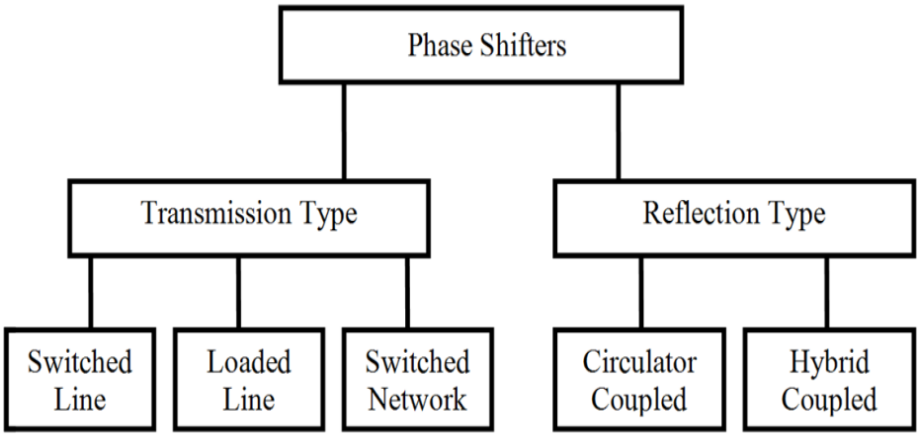

Figure 2-5 General Classification of Phase Shifters

2.3.1 Transmission Type Phase Shifter Circuits

2.3.1.a Switched-Line Phase Shifters

In switched line phase shifters, phase shift is created by switching between two transmission lines of different lengths.

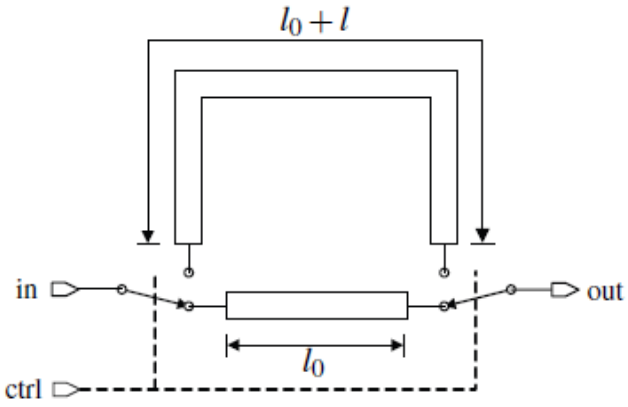

Figure 2-6 Switched-Line Phase Shifter

Differential phase shift formula of switched line topology of Figure 2-6 is given as follows

$$\Delta\emptyset = \emptyset_{\mathbf{1}} - \emptyset_{\mathbf{2}} = \beta \times ((l_0 + l) - l_0) = \beta l \tag{2.8}$$

where

$$Propagation\ Constant: \beta = \omega_c / \upsilon_P \tag{2.9}$$

ω_c: Center frequency

υ_P: Phase velocity

Δl: Difference between reference and difference line lengths

Equation 2.8 implies that phase difference is a function of frequency in switched line phase shifters. By this property, switched line phase shifters may be used as true time delay devices.

$$Time\ Delay: \Delta\tau = \Delta l / \upsilon_P \tag{2.10}$$

However, because of the same property, it is hard to expect wideband characteristic from switched line phase shifters as phase error tend to increase rapidly as phase shift is first order function of frequency.

Insertion loss is mainly determined by the loss of SPDT switches. Insertion loss of switches contributes to both paths almost equally. However, transmission lines of different lengths exhibit different insertion losses in each path and that causes amplitude imbalance. Amplitude imbalance is an undesirable effect in phase shifters as it contributes to phase imbalance.

2.3.1.b Loaded-Line Phase Shifters

In loaded line phase shifters, phase difference is created by changing the propagation characteristics of the transmission line by switching between shunt susceptances or series reactances as it is seen in Figures 2-7.a and 2-7.b.

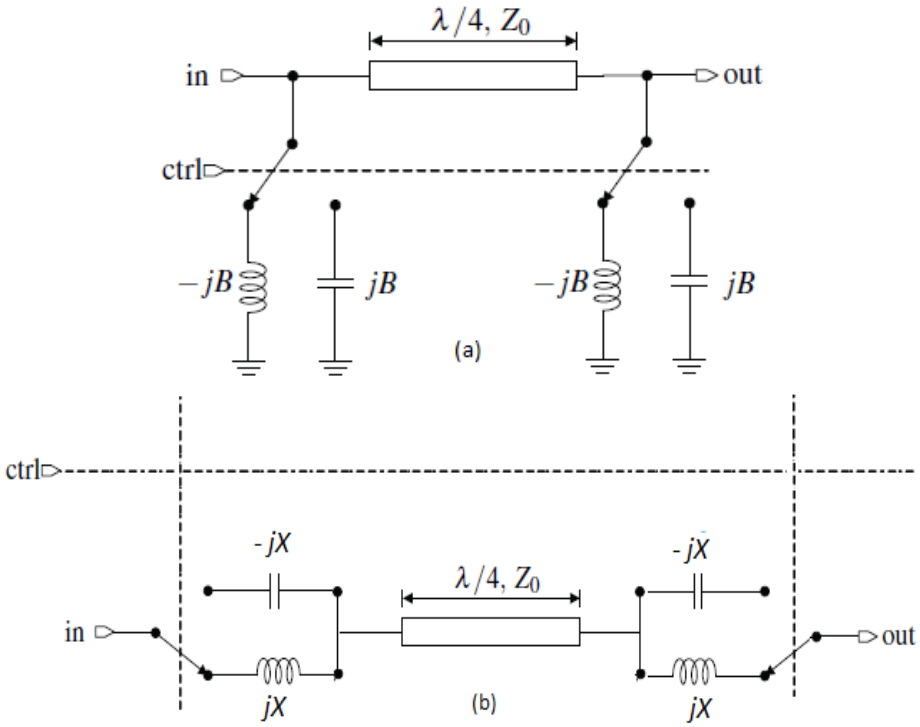

Figure 2-7 Loaded-Line Phase Shifters
(a)Shunt Susceptance Structure, (b) Series Reactance Structure

Transmission (ABCD) parameters can be utilized to analyze loaded line phase shifters as ABCD parameters makes matrix multiplication of cascaded stages possible [17]. ABCD parameters of all three stages are multiplied under maximum bandwidth condition which is $\theta=\pi/2$ and $B=B_1=-B_2$, for simplification [28].

$$T = \begin{bmatrix} 1 & 0 \\ jB & 1 \end{bmatrix} \cdot \begin{bmatrix} 0 & jZ_0 \\ j/Z_0 & 0 \end{bmatrix} \cdot \begin{bmatrix} 1 & 0 \\ jB & 1 \end{bmatrix} = \begin{bmatrix} -BZ_0 & jZ_0 \\ j(1 - B^2{Z_0}^2)/Z_0 & -BZ_0 \end{bmatrix} \quad (2.11)$$

Converting ABCD parameters back to S parameters, phase shift can be found as follows

$$\Delta\phi = 2\, tan^{-1}\left(\frac{B}{1 - 0.5B^2}\right) \quad (2.12)$$

Mathematically it is impossible to have phase shift values out of [-90º, 90º] interval which means maximum phase shift of loaded line phase shifters cannot be more than 180º. However this limit is reduced to around 45º in practice due to degradation of S_{11} and S_{22} characteristics with the growing phase shift values [28]. On the other hand, phase shift is proven to be independent of frequency in loaded-line phase shifters. This property implies that constant phase shift over a wide frequency range can be achieved with loaded-line phase shifters. The practical bandwidth is reported to be around 25%.

2.3.1.c Switched-Network Phase Shifters

High pass filter-low pass filter and all pass filter network based phase shifters are popular switching network phase shifter topologies whose principal of operation are very similar. Differential phase shift in HPF-LPF topology is provided by switching between a high pass and a low pass filter whereas switching is done between all pass filters in APF topology. In HPF-LPF topology, high pass filter part gives phase advance, while in contrast; low pass filter part gives phase delay. Eventually, circuit stays matched against frequency variation [17]. Due to the naturally matched feature, both HPF-LPF and APF topologies exhibit good return loss characteristic which permits an easy tuning over phase shift performance. By the proper choice of network element values, phase responses reference and difference paths of both HPF-LPF and APF topologies can be arranged to follow each other with a constant phase difference. Mathematical expressions for both topologies are given below. Normalized reactance and susceptance values are symbolized with X_n and B_n, respectively.

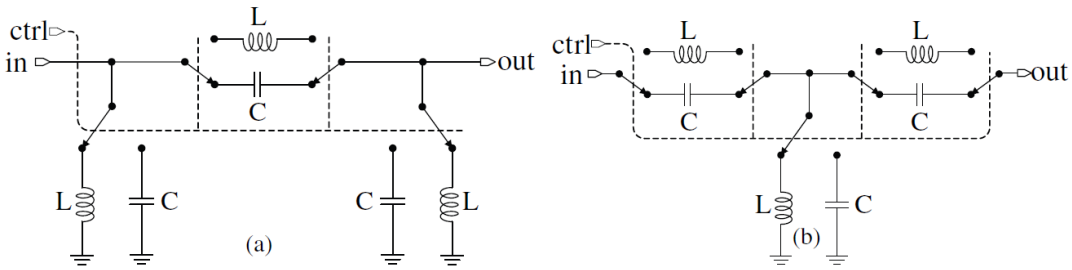

Figure 2-8 Configurations of High Pass Filter-Low Pass Filter Topology
(a) Π-type Configuration (b) T-type Configuration

Low Pass Filter Part LC values for Π-type network -90<Ø<0 (Figure 2-8.a)

$$L = \frac{Z_o \, sin|\emptyset|}{\omega_0} \tag{2.13}$$

$$C = \frac{tan|\emptyset/2|}{\omega_0 Z_o} \tag{2.14}$$

High Pass Filter Part LC values for Π-type network 0< Ø <90 (Figure 2-8.a)

$$L = \frac{Z_o}{\omega_0 \, tan|\emptyset/2|} \tag{2.15}$$

$$C = \frac{1}{\omega_0 Z_o \, sin|\emptyset|} \tag{2.16}$$

Low Pass Filter Part LC values for T-type network -90<Ø<0 (Figure 2-8.b)

$$L = \frac{Z_o \, tan|\emptyset/2|}{\omega_0} \tag{2.17}$$

$$C = \frac{sin|\emptyset|}{\omega_0 Z_o} \tag{2.18}$$

High Pass Filter Part LC values for T-type network 0< Ø <90 (Figure 2-8.b)

$$L = \frac{Z_o}{\omega_0 \, sin|\emptyset|} \tag{2.19}$$

$$C = \frac{1}{\omega_0 Z_o \, tan|\emptyset/2|} \tag{2.20}$$

Transmission (ABCD) matrix can be utilized to find differential phase shift of low pass filter part.

$$T = \begin{bmatrix} 1 & jX_N \\ 0 & 1 \end{bmatrix} . \begin{bmatrix} 1 & 0 \\ jB_N & 1 \end{bmatrix} . \begin{bmatrix} 1 & jX_N \\ 0 & 1 \end{bmatrix} = \begin{bmatrix} 1 - X_N B_N & j(2X_N - B_N {X_N}^2) \\ jB_N & 1 - X_N B_N \end{bmatrix} \tag{2.21}$$

By the help of expression 2.21, S_{21} can be found as

$$S_{21} = \frac{2}{2(1 - B_N X_N) + j\left(B_N + 2X_N - B_N {X_N}^2\right)} \tag{2.22}$$

Replacing $-B_N$ for B_N and $-X_N$ for X_N for HPF part, differential phase shift is found as

$$\Delta\phi = 2 \, tan^{-1}\left(-\frac{B_N + 2X_N - B_N {X_N}^2}{2(1 - B_N X_N)}\right) \tag{2.23}$$

Ideal situation implies that

$$|S_{21}| = 1 \tag{2.24}$$

Benefiting from formulas 2.22 and 2.24, susceptance is found as follows

$$B_N = \frac{2X_N}{1 + {X_N}^2} \tag{2.25}$$

Replacing 2.25 in 2.23 phase shift can be rewritten as follows

$$\Delta\phi = 2\,tan^{-1}\left(\frac{2X_N}{{X_N}^2 - 1}\right) \tag{2.26}$$

Using formulas 2.25 and 2.26, reactance and susceptance values can be expressed to be only dependent to differential phase shift value

$$X_N = tan\left|\frac{\Delta\phi}{4}\right| \tag{2.27}$$

$$B_N = sin\left|\frac{\Delta\phi}{2}\right| \tag{2.28}$$

Similar analysis for π-type circuit results in

$$X_N = sin\left|\frac{\Delta\phi}{2}\right| \tag{2.29}$$

$$B_N = tan\left|\frac{\Delta\phi}{4}\right| \tag{2.30}$$

Mathematical expressions of single and double stage APF structures are given below.

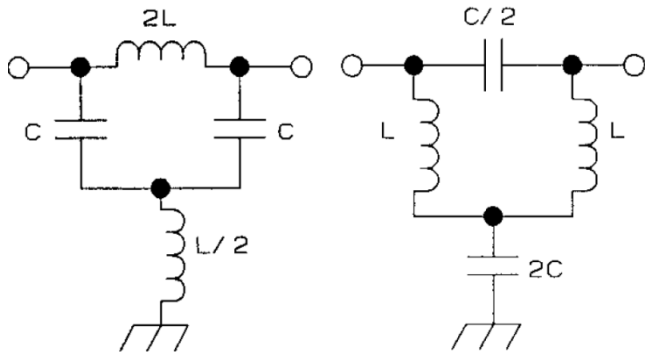

Figure 2-9 Series L and Series C Configurations of All Pass Filter Networks [24]

Reactance and susceptance values of the networks given in Figure 2-9 are

$$X = \frac{\omega L}{Z_0} \tag{2.31}$$

$$B = \omega C Z_0 \tag{2.32}$$

Calculations are simplified by using normalized impedance and frequency definitions

$$Normalized\ Impedance: z = \frac{1}{Z_0}\sqrt{\frac{L}{C}} \tag{2.33}$$

$$Normalized\ Frequency: \Omega = \frac{\omega}{\omega_0} \tag{2.34}$$

where ω_0 is transition frequency and it is calculated as follows

$$\omega_0 = \sqrt{\frac{1}{LC}} \tag{2.35}$$

Using equations 2.31-2.35 reactance and susceptance expressions can be rewritten as

$$X = \Omega z \tag{2.36}$$

$$B = \frac{\Omega}{z} \tag{2.37}$$

S parameters of frequency independently matched reciprocal and lossless circuit are

$$S_{12} = S_{21} = \frac{1}{2}(\Gamma_e - \Gamma_o) \tag{2.38}$$

$$|S_{21}| = 1 \tag{2.39}$$

$$S_{11} = S_{22} = 0 \tag{2.40}$$

where

$${Z_0}^2 = L/C \tag{2.41}$$

$$\Gamma_e = \frac{jWz - 1}{jWz + 1} \tag{2.42}$$

$$\Gamma_o = \frac{1 - jW/z}{1 + jW/z} \tag{2.43}$$

$$W = \Omega - 1/\Omega \tag{2.44}$$

Solving equations 2.33 and 2.41simultaneously gives

$$z = 1 \tag{2.45}$$

From the equations 2.38-2.45 following equation that is defining phase difference between input and output of the circuit can be obtained as

$$\psi = \pi - 2\,tan^{-1}(\Omega - \frac{1}{\Omega}) \tag{2.46}$$

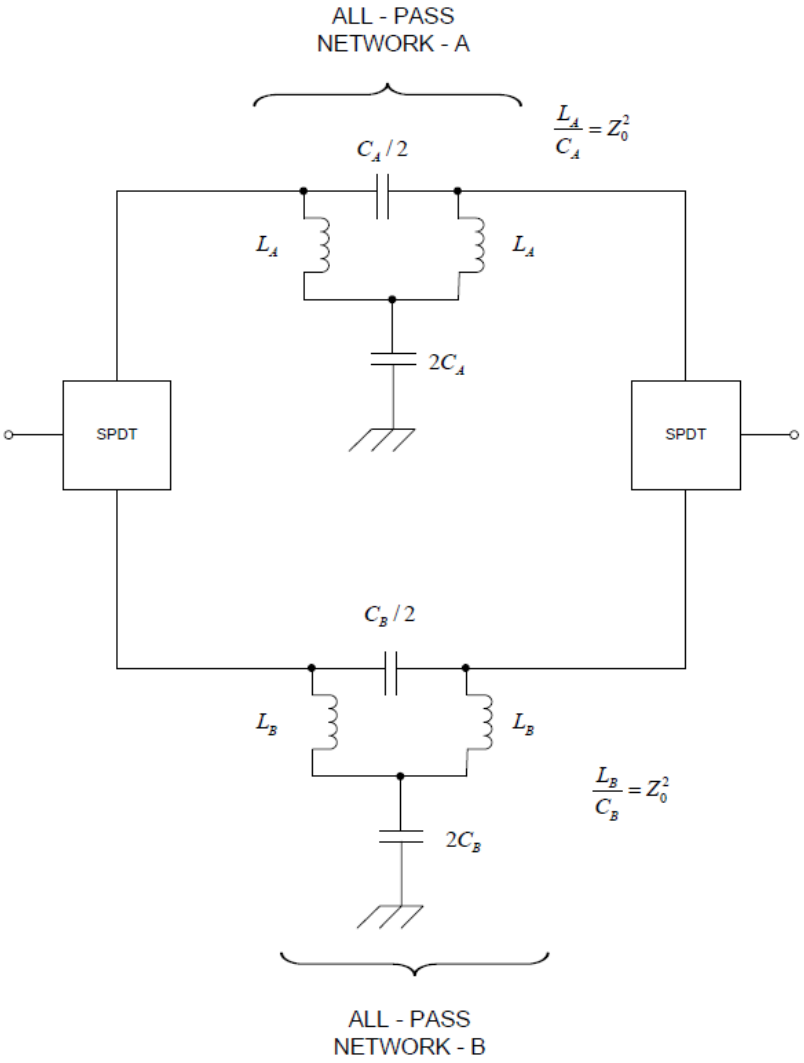

Figure 2-10 Single Stage All Pass Filter Based Phase Shifter

Figure 2-10 shows single stage APF based phase shifter structure. Phase shift is generated by switching between networks A and B whose transition frequencies are ω_A and ω_B respectively.

For simplicity, circuit transition frequency ω_m and design parameter p are introduced and normalized impedance Ω is redefined as follows

$$\omega_m{}^2 = \omega_A \omega_B \tag{2.47}$$

$$p^2 = \frac{\omega_A}{\omega_B} \tag{2.48}$$

$$\Omega = \frac{\omega}{\omega_m} \tag{2.49}$$

Phase difference of individual sections can now be expressed as follows

$$\psi_A = \pi - 2\,tan^{-1}(\Omega p - \frac{1}{\Omega p}) \tag{2.50}$$

$$\psi_B = \pi - 2\,tan^{-1}(\frac{\Omega}{p} - \frac{p}{\Omega}) \tag{2.51}$$

Hence differential phase is

$$\Delta\phi(\Omega) = \psi_A - \psi_B = 2\left\{tan^{-1}(\Omega p - \frac{1}{\Omega p}) - tan^{-1}(\frac{\Omega}{p} - \frac{p}{\Omega})\right\} \tag{2.52}$$

Design parameter p can be calculated as follows at the center frequency Ω=1

$$p = \frac{1}{2}tan\left(\frac{\Delta\phi}{4}\right) + \sqrt{1 + \frac{1}{4}tan^2\left(\frac{\Delta\phi}{4}\right)} \tag{2.53}$$

Now element values can be calculated by the help of p and ω_m values as follows

$$L_A = \frac{pZ_0}{\omega_m} \tag{2.54}$$

$$L_B = \frac{Z_0}{p\omega_m} \tag{2.55}$$

$$C_A = \frac{p}{Z_0\omega_m} \tag{2.56}$$

$$C_B = \frac{1}{pZ_0\omega_m} \tag{2.57}$$

Additionally peak-to-peak flatness $\epsilon(\phi)$ can be calculated by the following formula

$$\epsilon(\phi) = \phi\left(\Omega = \sqrt{\frac{\omega_{High}}{\omega_{Low}}}\right) - \phi_0 \tag{2.58}$$

2.3.2 Reflection Type Phase Shifter Circuits

Reflection type phase shifter circuits use reflective terminations. In a digital reflection type phase shifter, desired phase shift value can be produced by switching between proper terminations. In general, reflection type digital phase shifters consist of three divisions which are body network (e.g. circulator or coupler), switching network and termination network. Reflection type phase shifters are named according to the body network. Most famous reflection type phase shifters are hybrid coupler based and circulator based phase shifters. Either PIN diode or FET switching may be used for digital phase shift operation. In design process, switching network should be designed carefully and switch characteristics should be included in analysis.

Reflected power to the incident power ratio is $|\Gamma|^2$ in both circuits of Figure 2-11. Based upon the fact that $|\Gamma| = 1$ in ideal case, there is no loss in the system power as all the power is reflected back to system from the reflecting terminations. If reflection coefficients of two states are represented as $\Gamma_1 = |\Gamma_1|\angle\phi_1$ and $\Gamma_2 = |\Gamma_2|\angle\phi_2$, then the differential phase shift is found as $\Delta\phi = \phi_1 - \phi_2$ [41].

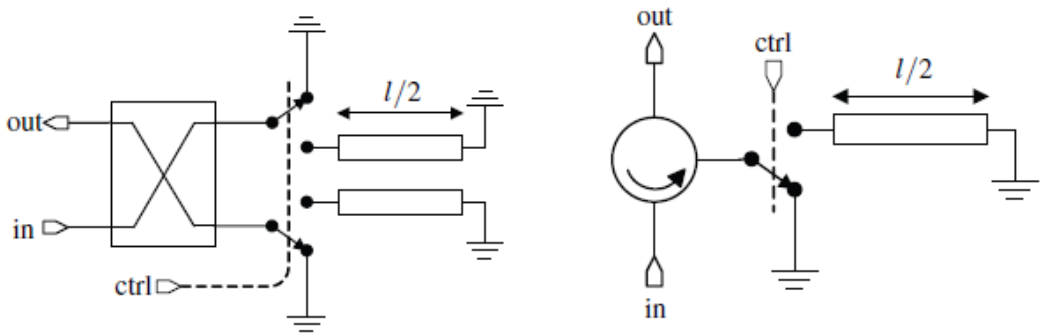

Figure 2-11 Reflection Type Phase Shifter Circuits
(a) Hybrid Coupler Based, (b) Circulator Based

In Figure 2-11.a, hybrid coupler based phase shifter is given. 3dB 90º hybrid coupler based phase shifter divides the power incident at the excitation port equally to thru port and coupled port with 90º phase difference between them. After these two signals are reflected back from the identical terminations, they add up at normally isolated port with adjusted phase difference while cancelling at excitation port.

In Figure 2-11.b Directionality property of circulator is used. In circulator based phase shifter, incident signal from excitation port comes out with a phase difference at the output port after being reflected by the terminated port.

Even though one termination circuit and one switch more than circulator based phase shifter is needed in hybrid coupled phase shifters, they are generally more preferable to circulator based phase shifters due to their low loss, low cost and low volume properties. Besides, they are easier to fabricate and more prone to MMIC design.

Both hybrid coupler and circulator based phase shifters are well-matched devices. However, termination networks that are added to generate the desired phase shift value may cause mismatching problems. Termination network can be either a transmission line that has half of the electrical length of the desired phase shift value or a circuit consisting of lumped elements.

A very compact termination circuit is proposed in [17]. It is reported that any required phase shift value is realizable for octave band operation. Performance of the phase shifter network depends mainly on quality of the body network.

CHAPTER 3

DESIGN and FABRICATION OF PCB PHASE SHIFTERS

3.1 General Design Process for PCB Phase Shifters

General design process for a phase shifter is given in Figure 3-1. A phase shifter design starts with determining the design requirements. After that conceptual requirements should be converted to numerical values and ranked according to their importance in design. This ranking is done by assigning weighting coefficients to the requirements. In this thesis, transmission line type is chosen according to ease of manufacture and production technology is selected in accordance with the available laboratory facilities. Then, other components such as switching elements, connectors and lumped elements that are appropriate for the selected technology process are chosen. After that, a phase shifter topology is selected and analyzed in any of the proper design environments. Once the satisfactory simulation results are achieved, final design is realized and measured. Design requirements may need to be reconsidered if the results are not satisfactory. In this case, if possible, it would be wise to relax the "problematic" requirement by modifying other parts of the RF stripe. Secondly, if the requirements are met, studies and experiments should be documented.

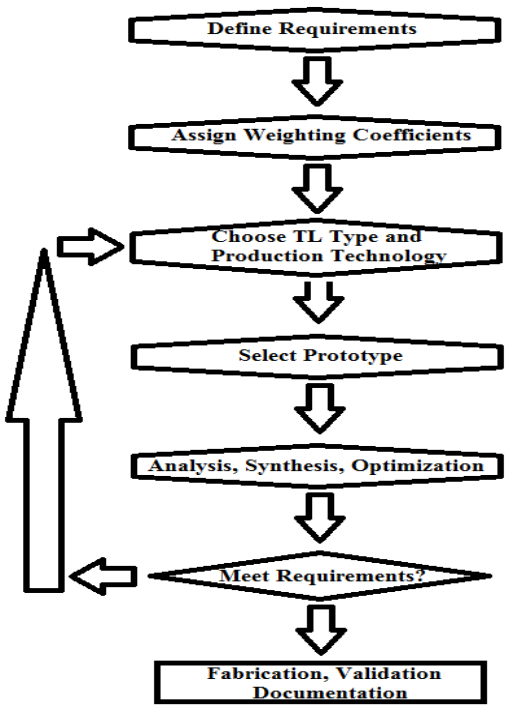

Figure 3-1 General Design Procedure of PCB Phase Shifters

3.1.1 Weighting of Design Requirements for Investigated Phase Shifter Circuits

Importance of a parameter in a design is indicated with requirement weighting planning. Weighting coefficients must be assigned accurately as this planning affects trade-off design. For the weighting of design requirements of circuits designed in this thesis, 1-10 point scale is used where 10 point is given to the most important design criteria.

Table 3-1 Weighting of Design Requirements for the Investigated Phase Shifter Circuits

Phase Shifter Network Requirements		Weighting Coefficient
Operating Frequency Range	**widest possible bandwidth guaranteeing 2-4GHZ operation**	**10**
Differential Phase Shift and Peak to Peak Phase Error	**90°±5°**	**10**
Peak to Peak Amplitude Imbalance	**≤1dB**	**8**
Input and Output Return Loss	**≤-10 dB**	**6**
Insertion Loss	**≤2dB**	**4**

First and second steps of the flowchart are applied as in Table 3-1. Circuits with widest possible bandwidth guaranteeing 90°±5° operation in S-Band with less than 10dB return loss, 1dB peak to peak amplitude imbalance and 1.5 dB insertion loss are aimed to be realized.

3.1.2 Selection of Transmission Line Type, Production Technology and Substrate

In this study, ease of design and manufacturing is the primary factor in selection of transmission line type. Various types of transmission lines are compared in detail in [44]. Strip-line and slot-line offer bad mounting for series connections. Coplanar waveguide offers great ease of mounting for circuit components Microstrip-line design offers bad shunt element mounting however it also offers better ease of manufacture than coplanar waveguide design. Therefore, in this thesis, coplanar waveguide design is preferred where shunt mounting is necessary, if not; microstrip design is preferred due to ease of layout formation.

Various production technologies are introduced in [44]. Technology process includes conductor material selection, dielectric material selection, layer quantity and connection between layers decision. Monolithic design is suitable for low power applications. Thick film technology has poor integration level while thin film is an expensive technology. Although PCB technology has these disadvantages at a moderate level, it is more preferable as it is cheap and easy to fabricate. LTCC offers good tolerance, high integration level and frequency stability at a reasonable cost. What is more, it has good thermal conductivity and hermetic packaging feature. All these advantages make them superior over PCB technology. Nonetheless PCB technology is preferred in this thesis due to the available laboratory facilities.

Increasing the dielectric constant and substrate height increases the surface wave radiation effects, hence coupling effects between neighboring paths. On the other hand, high dielectric constant and low substrate height cause small line widths. In [44], it is stated that increasing the substrate height results in less conductor loss and better tolerance value. However, it also leads to higher radiation and greater via-hole parasitic inductance. Decreasing the dielectric constant increases the circuit size due the increment in transmission line lengths. Additionally, substrate should have high uniformity. Conductor loss due to the skin depth problem can be reduced by selecting 3 to 5 times thicker conductor than the skin depth. Copper is a low loss, frequency stable material with high conductance value. Even though gold is more resistant to corrosion effects, there is a significant price difference between two materials. Taking into account the information that skin depth of copper is about 1.1um at 4GHz, all 1/2, 1 and 2 oz metal thickness options are appropriate for the circuits designed in this thesis.

Considering the stated facts, a substrate that offers moderate height and dielectric constant is selected. Additionally, considering the available laminates at ASELSAN stocks, RO4000 Series Laminates with $\varepsilon_r \approx 3.62\text{-}3.72$ between 1.5-6GHz, RO4003, 1/2oz Cu 20 mil is preferred for the circuits investigated in this thesis.

3.1.3 Selection of Switches, Driving Circuitry, Lumped Elements and Connectors

Switching elements are not used in this thesis. Instead, reference and difference paths are connected in turn and phase responses of two paths are compared. However, it would be handy to touch on some basic knowledge. No matter FET or PIN diode (see section 2.2.6) switching is selected, all ports of the switching elements should be well isolated from each other in order to suppress surface wave radiation based coupling effects and to have good signal discrimination. Selecting a switch with non-reflective property is more preferable and return loss values of all states of the switch should be as good as possible. Also, driving circuit design should be carried carefully. A basic method to feed the switches with a clean supply is to mount a shunt capacitance close to the switching element. Furthermore, assembling DC blocking capacitances of switching elements should not be forgotten.

Amplitude and phase imbalance between outputs of the switch should be very low. In multibit phase shifter design, low loss switches should be preferred. Cost reduction is very important in PAR applications where thousands of T/R modules are employed.

In this thesis, lumped element tolerance value is the primary property in lumped element selection. In designs where many COTS components are employed, tolerance value should be as low as possible. SRF value of inductors determines the upper design frequency meanwhile having high quality factor is very important as it affects operational bandwidth. Especially inductor package selection is crucial as smaller package offers high quality factor, less parasitic effects, smaller size and wider range of inductor values. This is a good reason for selecting 0201 package instead of 0603 package. However 0201 package is very difficult to assemble on the PCB. Considering the above factors, Coilcraft's 0402CS series 2% tolerance C328-A2 kit inductors, AVX's 0402 Package ±0.02pF tolerance ACCU-P0402KIT01 kit capacitors for values below 2pF and ATC's 0402 Package ±0.1pF tolerance ATC KIT 37T-600L series capacitors for values above 2pF are selected for every implemented circuit in this thesis. An easy to mount, short and thin pin RF connector providing up to 18GHz operation is selected for designed circuits.

3.1.4 Selection of Prototype Circuit and Analysis

Two-stage all pass filter based phase shifter, eight-element loaded-line phase shifter, aperture coupler based phase shifter and shunt stub phase shifter circuits are investigated in this thesis. 90° phase shifters covering S-Band with widest possible bandwidth without sacrificing from the other requirements stated in Table 3-1 are intended to be designed. Experiments and results are tabulated in Section 3.3. For the analysis of circuits, AWR® is used for simulation and optimization of all pass filter based phase shifter, loaded-line phase shifter and shunt stub phase shifter. HFSS™ is used for simulations of aperture coupler based phase shifter. MATLAB® is utilized for calculation of lumped element values of the all pass filter. Final enhancements are made by optimizations in accordance with the design requirements given in Table 3-1.

3.2 Fabrication of Selected Phase Shifter Topologies

For each circuit of this thesis, once the final design is satisfactory, circuits are manufactured using LPKF Protolaser 200 and Protomat H100 PCB prototyping machines. Firstly, via holes are drilled in Protomat H100. After the via hole coating process, Protolaser 200 is used for sketching the pattern. Protolaser tolerance is reported to be 0.02 mils. Such an amazing property is important in sketching high impedance, hence low width transmission lines where tolerance value gets proportionally worse. Agilent N5230A 10MHz-40GHz PNA-L network analyzer is calibrated via SOLT method between 1-8GHz with Rohde Schwarz 85052B 3.5mm, dc-26.5GHz calibration kit. Measurement results are given in comparison with simulation results for validation of circuits. Fabrication and measurement processes of selected circuits are explained in detail in following sections.

3.2.1 Two-Stage All Pass Filter Based Phase Shifter

Mathematical expressions for all pass filter based phase shifter are given in sections 2.3.1.c and Appendix B.

For the second order analysis of cascaded all pass phase shifter given in Figure 3-2, third design parameter q is introduced as follows

$$q = \sqrt{\frac{\omega_{A2}}{\omega_{A1}}} = \sqrt{\frac{\omega_{B2}}{\omega_{B1}}} \tag{3.1}$$

Phase shift value of two-stage all pass filter based phase shifter can be calculated by the following formula

$$\frac{\Delta\phi}{2} = tan^{-1}\left(\frac{\Omega}{pq} - \frac{pq}{\Omega}\right) - tan^{-1}\left(\frac{\Omega p}{q} - \frac{q}{\Omega p}\right) + tan^{-1}\left(\frac{\Omega q}{p} - \frac{p}{\Omega q}\right) - tan^{-1}\left(\Omega pq - \frac{1}{\Omega pq}\right) \tag{3.2}$$

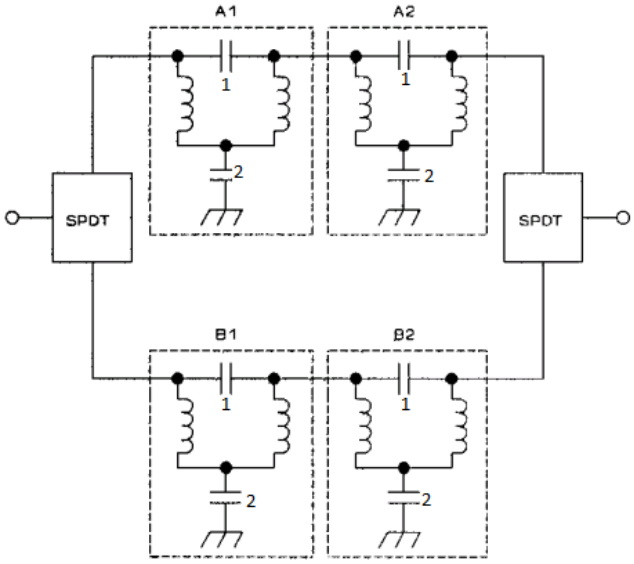

Figure 3-2 Locations of Sections and Lumped Elements in Two-Stage All Pass Filter [24]

Bandwidth of the structure is limited due to the non-distributed characteristics of COTS components. Because of the same reason, pure all pass filter characteristics cannot be maintained over the operational bandwidth. Therefore, electrical performance of COTS components should support the design band. COTS components should have low variation in their values, high quality factor and sufficient SRF value in order to have good phase and amplitude responses.

MATLAB® code given in Appendix C is developed to automate calculation of the least phase error giving p, q and Ω parameters. These parameters are transferred to AWR® design environment to calculate and assign capacitor and inductor values. After many trials, it is experienced that in order to design a phase shifter covering whole S-Band, the best option is to use p and q parameters of a 1.8-5.4GHz phase shifter whereas selecting Ω≈1.15 as center frequency of the phase shifter tends to shift to left side of the spectrum. What is more, this selection covers two suggestions given in [24]. First advice is design bandwidth versus tolerance value consideration of lumped elements. If maximum tolerance value is t, lower and upper design frequencies should be f_{low_design} =(1-t)* $f_{low\_required}$ and f_{high_design} = (1+t) *$f_{high\_required}$, respectively. Even though t=0.02 for the selected kits, 1.8-5.4GHz selection is even suitable for 10% tolerance value. However, amplitude and phase response repeatability decrease with the tolerance value. Second suggestion is to carry transition frequencies w_{center}/(pq) and w_{center}*(pq) out of the desired design band as high amplitude imbalance at these points result in high phase error in phase shift response. This is also handled by preferred design frequency selection.

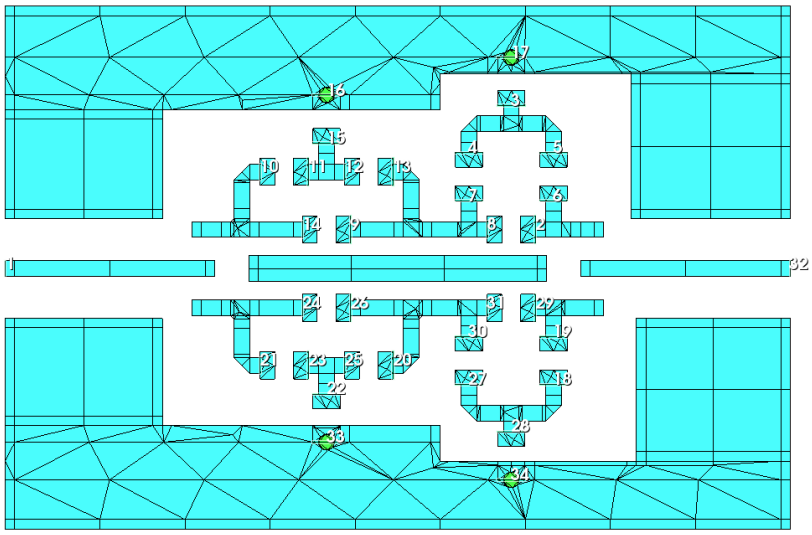

Figure 3-3 Formed Layout of Two-Stage All Pass Filter

Layout given in Figure 3-3 is formed for the design Reference and difference paths should be equal in layout formation in order not to increase amplitude and phase imbalances. Framing ground plane and EM interactions over the layout spoil the phase response. Lumped element values are tuned to correct the spoiled phase response while keeping return loss value at an acceptable level.

In lumped element tuning process, firstly, inductors of theoretical values are replaced with the ones that are close to them in value but have higher quality factor and lower deviation in their inductance value. This can be done since phase response is already spoiled by the addition of the layout and phase and amplitude responses can be corrected by proper tuning of capacitor values in both cases. After inductor values are assigned and their S-parameters are buried into simulation of the design, final tuning is done over capacitor values and the circuit is prepared for fabrication. EM simulation results of these two steps and the phase response of the fabricated circuit are given together in Figure 3-4.

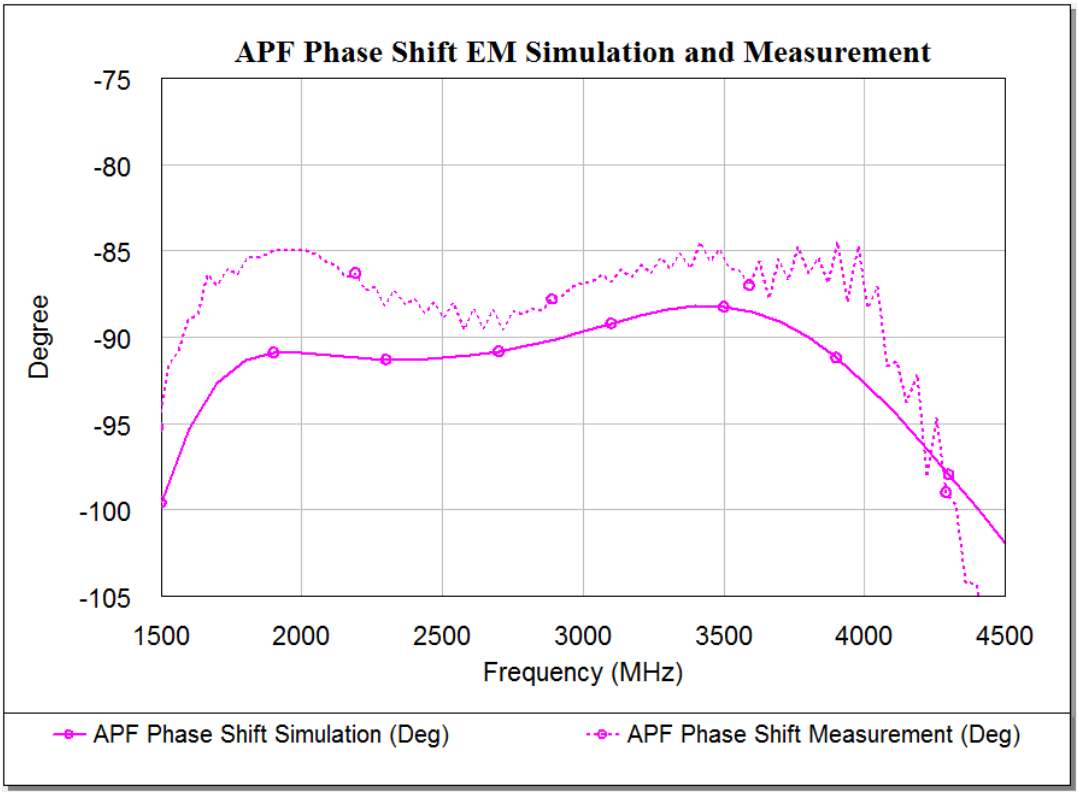

Figure 3-4 All Pass Filter EM Simulation and Measurement of Phase Shift

EM simulation of the linear circuit with the formed layout has 83.5°±5° phase shift response between 1700 and 4000MHz. Tuned lumped element values over the same layout exhibits 93°±5° within the 1550-4250MHz band. Finally, fabricated circuit has 90°±5° phase shift performance within the 1500-4200MHz band. In general, simulation and measurement results exhibit good accordance.

Theoretical values and final values of inductors and capacitors of each section are given in Table 3-2. Allocation of the elements can be reviewed in Figure 3-2.

Table 3.2 APF Theoretical and Optimized Values of Lumped Elements

L[nH],C[pF]	Theoretical	Optimized
LA1_1=LA1_2	4.65	4.3
LA2_1=LA2_2	1.93	2.2
LB1_1=LB1_2	1.40	1.8
LB2_1=LB2_2	3.38	3.6
CA1_1	0.93	1.1
CA1_2	3.72	4.7
CA2_1	0.39	0.4
CA2_2	1.54	1.5
CB1_1	0.28	0.2
CB1_2	1.12	1.2
CB1_1	0.68	0.8
CB1_2	2.71	2.7

Bandwidth is wider when inductors of neighboring stages are placed perpendicularly to each other instead of being placed parallelly. This is obviously because the cancellation of some of the coupling effects that are caused by the radiation of inductors. Layouts of reference and difference paths should be formed equally not to increase amplitude and phase imbalances. Additionally, transmission lines should be as short as possible for similar reasons and also for compactness.

Once the satisfactory results are obtained, designed circuit is realized using laser prototyping machines. Afterwards, lumped elements and connectors are mounted on the fabricated PCB and the circuit is measured. Amplitude responses of designed and fabricated circuits are given in Figure 3-5.

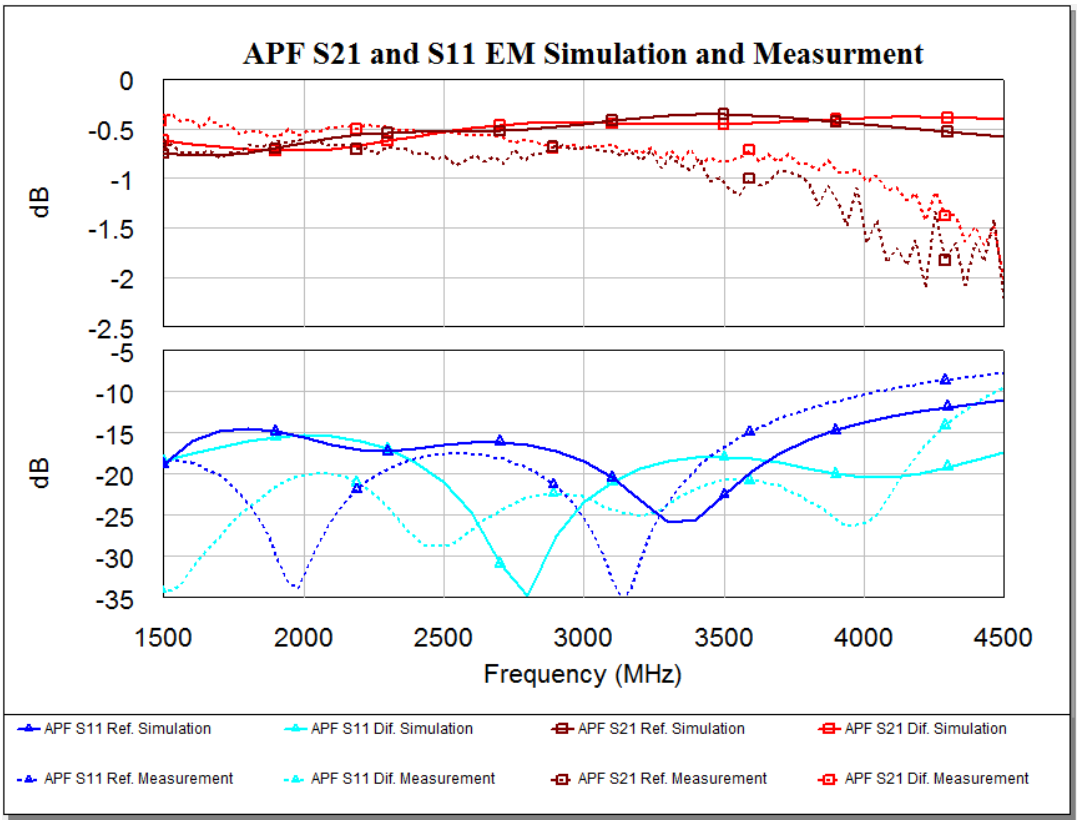

Figure 3-5 S_{21} and S_{11} Characteristics of Designed and Fabricated All Pass Filter Circuit

Insertion loss and amplitude imbalance criterion are achieved as the S_{21} parameter of the circuit varies between 0.3-1.5dB for both states through the S-Band.

Return loss is better than 10dB for all states in the whole S-Band. 10dB return loss may not be sufficient in multibit design as cascaded return loss tends to decrease. However, return loss may be improved by adding attenuators to the both ends of the circuit. These attenuators are expected to improve the return loss of the added side (either input or output) by double amount of its value. Nevertheless, in such a solution, in the receiver part signal to noise ratio degradation problem due to the increment in noise figure of the system; in the transmitter part, heat-sink problem in parallel with amplifier requirement may arise.

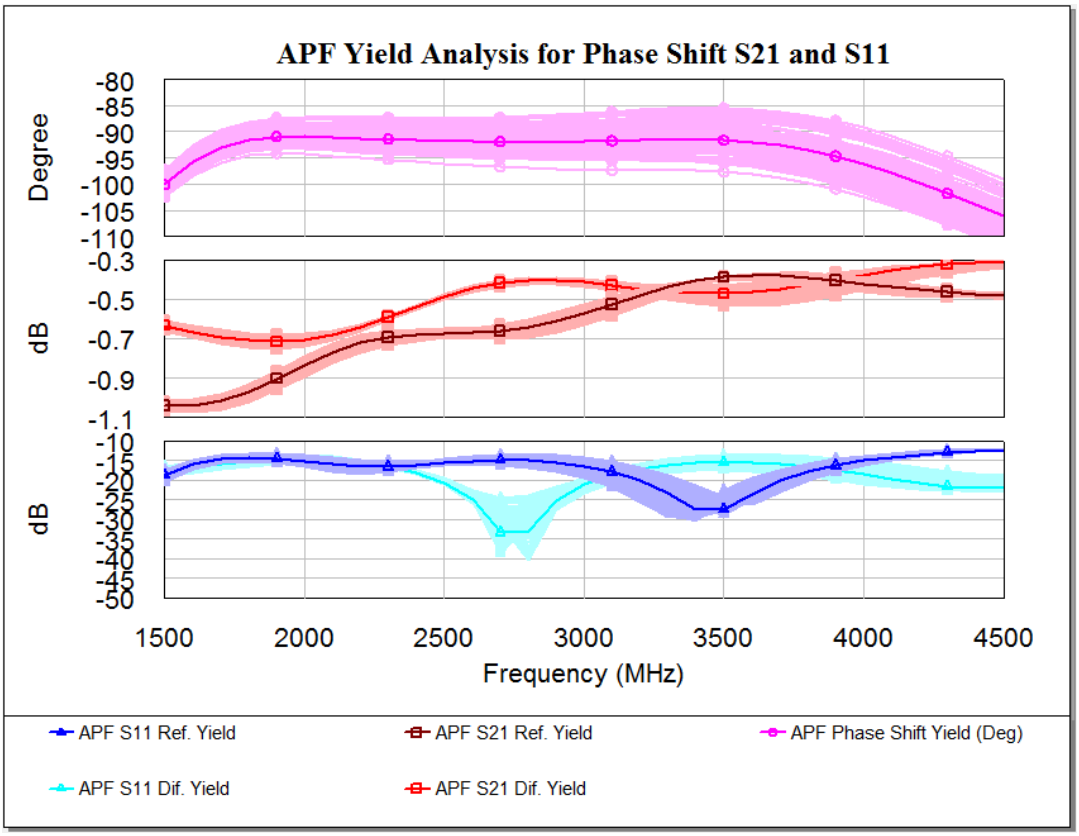

Figure 3-6 Yield Analysis of Designed All Pass Filter Circuit

Figure 3.6 demonstrates how difficult to repeat the same phase response. However ±5° difference between repeated circuits is acceptable considering the desired phase error performance. Even soldering dust spoils the response where many elements are soldered. It is experienced that phase response of all pass filter based phase shifter is very dependent on lumped element values and transmission line lengths. Good tuning over inductor and capacitor values or transmission line realization for lumped elements is required to overcome this drawback.

Necessity of intermediate inductor and capacitor values is the main drawback of all pass filter based phase shifter topology. Additionally, very small value lumped elements that are necessary in wideband or high frequency or small phase shift design may not exist in the market. There are two solutions to these problems. First one is to have manufacturers produce intermediate value lumped elements. Nevertheless cost of the circuit will probably be high in that option. Other solution is to realize capacitors and inductors in transmission distributed nature. However using interdigital capacitors and spiral inductors will enlarge the occupied area and increase the complexity of the circuit.

Figure 3-7 Fabricated Two-Stage All Pass Filter Circuit

Fabricated circuit occupies an area around 2cmx1cm. It can be counted as an advantage that all phase bits up to 180° are realizable by mounting the proper inductor and capacitor values onto the same layout. For a multi-octave operation, MIC design should be preferred as elements' non-distributive properties are conserved better in MIC technology [24].

3.2.2 Eight-Section Loaded-Line Phase Shifter

Conventional loaded-line phase shifter explained in section 2.3.1.b is insufficient for large phase shift bits especially in octave band design as load susceptances increase with the phase shift value and that yields a bad matching response. In order to cope with this problem, multiple loading sections can be utilized to share loading of the whole circuitry. However, this leads to a huge size and necessity of a large number of loading and switching elements [28]. Reactive elements are seperated from each other by a quarter wavelenght transmission line section to cancel reflections of the loading elements.

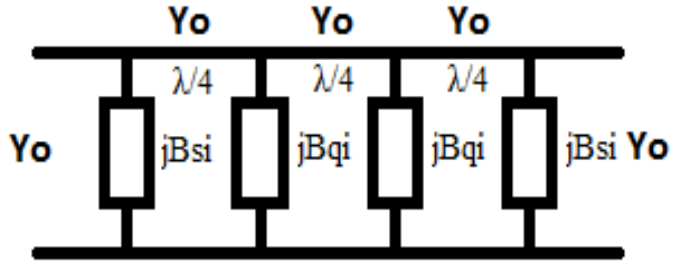

Figure 3-8 Schematic View of Four-Section Loaded-Line Phase Shifter

Element values of a four-section loaded-line phase shifter given in Figure 3-8 can be calculated by utilizing cascaded transmission (ABCD) parameters which is given as

$$\begin{bmatrix} A & B \\ C & D \end{bmatrix} = \begin{bmatrix} Z_0\left(B_{si} + B_{qi} - B_{si}{B_{qi}}^2{Z_0}^2\right) & j{Z_0}\left({B_{qi}}^2{Z_0}^2 - 1\right) \\ j{Z_0}\left({B_{si}}^2 - {B_{si}}^2{B_{qi}}^2{Z_0}^2 + 2B_{si}B_{qi} - {Y_0}^2\right) & Z_0\left(B_{si} + B_{qi} - B_{si}{B_{qi}}^2{Z_0}^2\right) \end{bmatrix} \quad (3.3)$$

Using the input match condition that is

$$BY_0 = CZ_0 \quad (3.4)$$

following equation can be written

$${B_{qi}}^2\left({B_{si}}^2{Z_0}^2 + 1\right) = 2B_{si}B_{qi} + {B_{si}}^2 \quad (3.5)$$

Transmission response of the loaded line phase shifter is as follows

$$S_{21} = |S_{21}|e^{j\emptyset} = \frac{1}{A + BY_0} \quad (3.6)$$

and yields

$$S_{21} = \frac{1}{Z_0\left(B_{si} + B_{qi} - B_{si}{B_{qi}}^2{Z_0}^2\right) + j\left({B_{qi}}^2{Z_0}^2 - 1\right)} \quad (3.7)$$

Using Equation 3.7 and setting B_{s1}= -B_{s2} and B_{q1}= -B_{q2} for simplification, differential phase shift can be expressed by the following formula

$$\Delta\emptyset = 2tan^{-1}\left|\frac{{B_{qi}}^2{Z_0}^2 - 1}{Z_0\left(B_{si} + B_{qi} - B_{si}{B_{qi}}^2{Z_0}^2\right)}\right| \quad (3.8)$$

For $\Delta\emptyset = 45°$ Equations 3.5 and 3.8 are solved simultaneously in MATLAB®. After that, capacitor and inductor values and transmission lengths are tuned in linear simulation. Theoretical and optimized values of lumped elements and transmission line lengths are given in Table 3-3.

Table 3-3 LL Theoretical and Optimized Values of Lumped Elements and TL Lengths

	Theoretical@MATLAB L[nH], C[pF], TL[mil]	Optimized@EM L[nH], C[pF],TL[mil]
C_s	**0.38**	**0.3**
L_s	**7.35**	**15**
C_q	**0.83**	**0.2**
L_q	**3.38**	**15**
TL	**580**	**660**

SRF value of 15nH is 3.28GHz. As the SRF is not exceeded much for S-band design, capacitance value in parallel with the inductor does not grow much. However for at higher frequency designs, SRF value should be taken seriously.

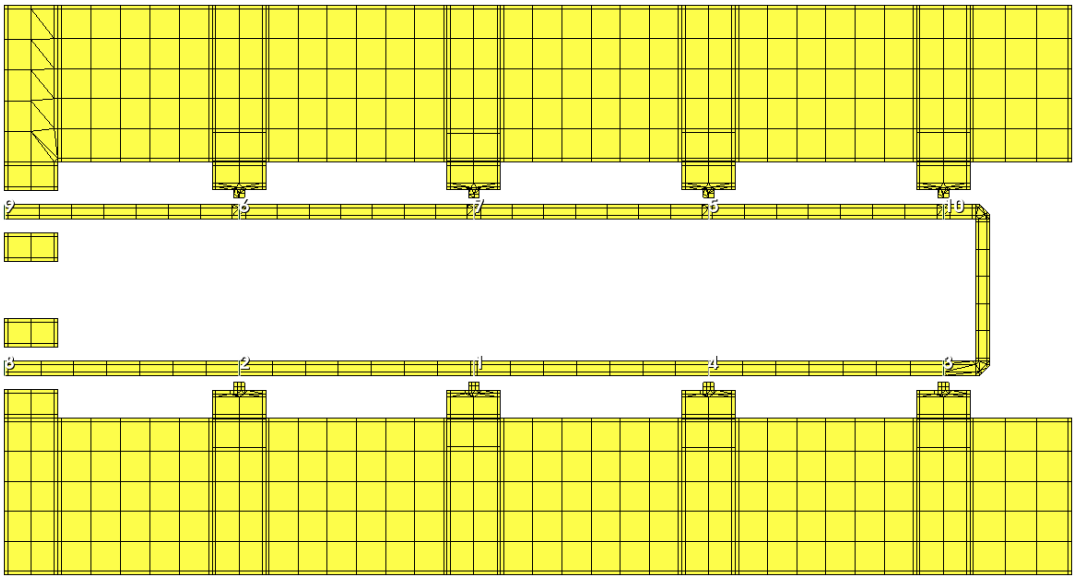

Figure 3-9 Formed Layout of Eight-Section Loaded-Line Phase Shifter

For the EM analysis of the obtained values, layout given in Figure 3-9 is formed. Every susceptance section in Figure 3-9 provides around 11.25° phase shift at a good matching level.

Figure 3-10 shows that simulated circuit exhibits 90°±5° phase performance within 2000-4150MHz band. On the other hand, fabricated circuit has 95°±5° phase shift performance in 1970-4000MHz band.

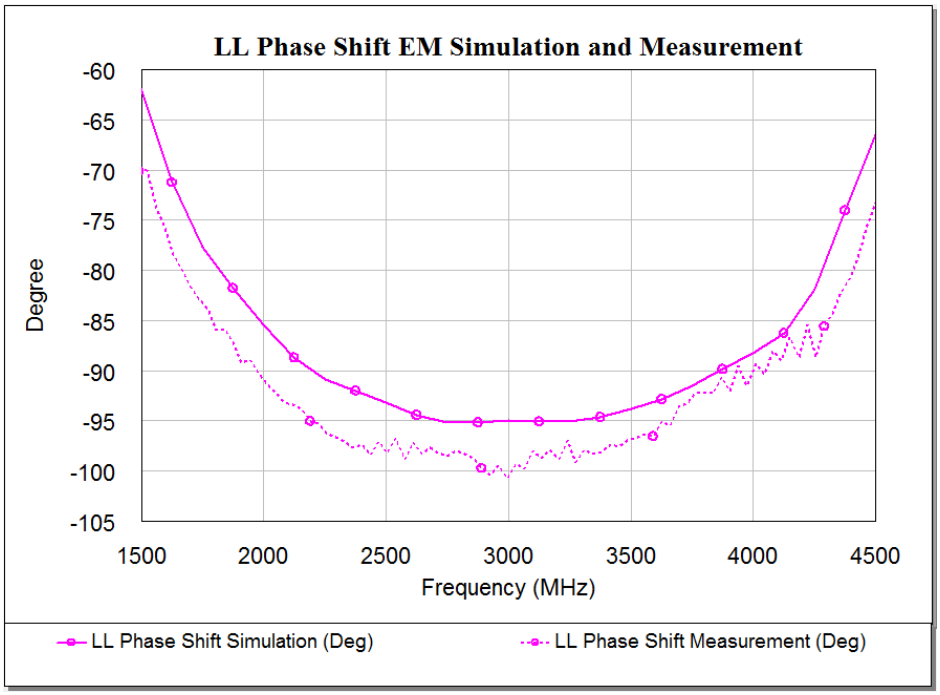

Figure 3-10 Loaded-Line EM Simulation and Measurement of Phase Shift

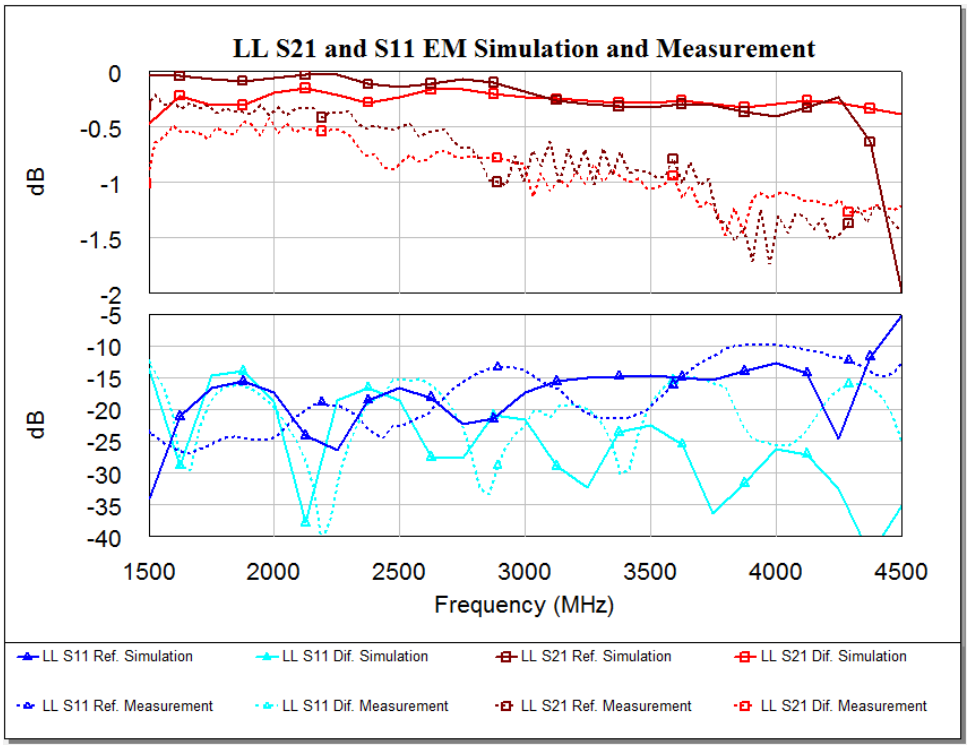

Figure 3-11 S_{21} and S_{11} Characteristics of Designed and Fabricated Loaded-Line Circuit

Amplitude responses of simulated and fabricated circuits are given in Figure 3-11. Transmission loss of simulated circuit is 0.2±0.2dB whereas that of the fabricated one is 1±0.7dB for all states within 2000-4000MHz band. Additional loss and amplitude variation between designed and fabricated circuit is caused by the addition of connectors due to connectors' increasing insertion loss with respect to frequency. Additionally, soldering process may have contributed to this undesired effect. Worst case return loss for all states is better than 13dB in simulation and better than 10dB for the manufactured circuit, for all states. These results ensure good matching characteristic. In general, results verify that there is a good coherence between results of designed and fabricated circuits.

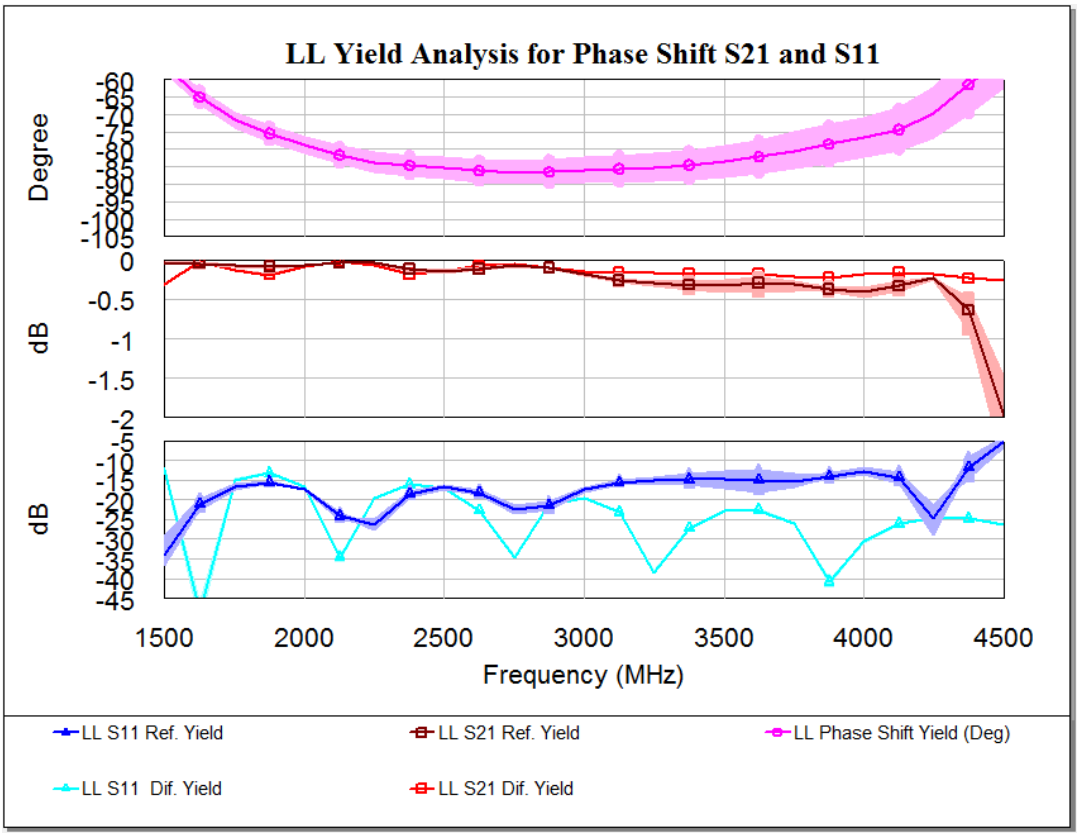

Figure 3-12 Yield Analysis of Designed Loaded-Line Circuit

2% inductor tolerance and ±0.02pF capacitor tolerance values are introduced for lumped elements in order to inspect the repeatability of the circuit. Yield analysis is run for 100 iterations and results are satisfactory as phase response is kept around ±5° whereas variations of amplitude parameters are negligible. This may yield an insufficient repeatability.

Generally PIN diode switching is preferred in loaded-line phase shifter design as it offers finer tuning over the response. However, results show that SPDT switches may be used when low tolerance-low variation lumped elements are utilized in design. This may reduce driving circuit complexity as the voltage leveling circuits are cleared from the circuitry. Whichever switching is used, number of switching elements will be considerably high. With basic math, 4-bit phase shifter with 360° coverage requires 30 switches in octave band loaded-line phase shifter design. This may bring size, cost and circuit complexity problems. This is the main drawback of the loaded-line phase shifter in front of using them in octave band PAR applications.

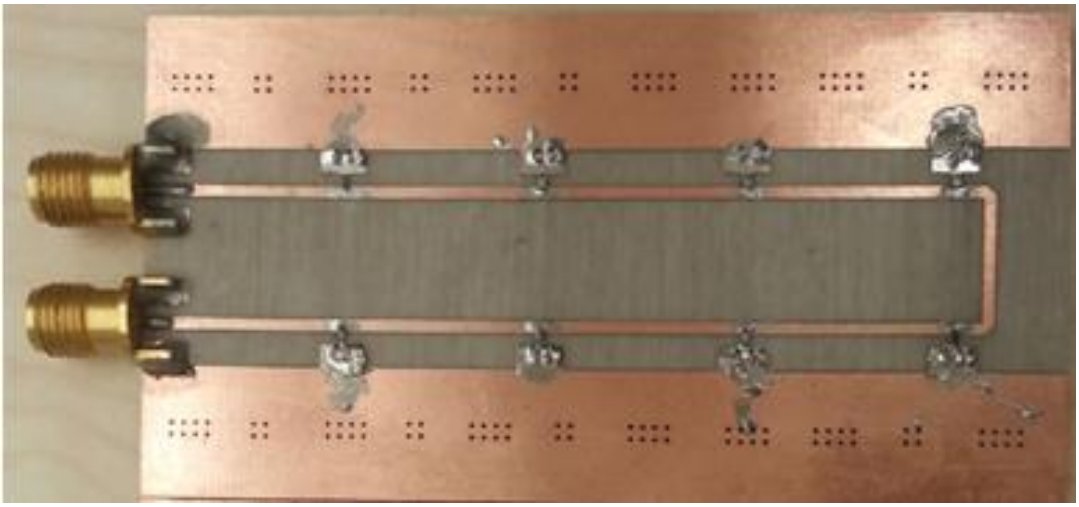

Figure 3-13 Fabricated Eight-Section Loaded-Line Circuit

Size of the fabricated circuit is around 7cmx4cm, however it could be at least around 2cm shorter in longer edge, due to the contribution of the exterior transmission lines to matching characteristic is negligible. Size of the circuit can be further reduced by using a higher dielectric substrate and bending the transmission lines. Cleanness of the soldering is very important where many components are soldered to the PCB.

3.2.3 Aperture Coupler Based Phase Shifter

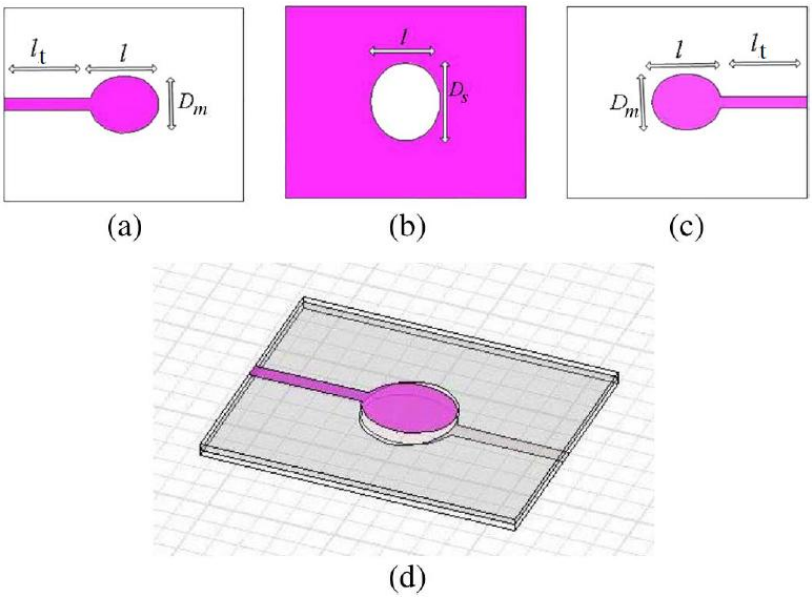

Figure 3-14 Configuration of Aperture Coupler Based Phase Shifter [16]
(a) Top Layer, (b) Mid-Layer, (c) Bottom Layer, (d) Whole structure

As shown in Figure 3-14, aperture coupler based phase shifter consists of three-layers that are: top, middle and bottom layers. In fact, it has four ports two of which is open circuited. In PCB technology, it can be realized by sticking two laminates on end. In order to achieve broad band tight coupling between patches, top and bottom patch major axes diameter D_m, mid-layer slot major axes diameter D_s and coupling length value should be calculated precisely. After that, reference microstrip line length l_{ref} should be calculated and tuned in order to have the desired phase shift value. A set of equations are given below for the calculation of the dimensions of the geometry.

Phase shift between the input and output ports of an aperture coupler that has a coupling value of C between its top and bottom patches is given by the following formula

$$\emptyset_c = 90° - 2\arctan\left[\frac{tan(\beta_{ef} l)}{\sqrt{1-C^2}}\right] \tag{3.9}$$

where

$$\beta_{ef} = 360° \times \frac{\sqrt{\varepsilon_r}}{\lambda} \tag{3.10}$$

$$\lambda = \frac{c}{f_c} \tag{3.11}$$

β_{ef} : Effective phase constant of the coupled structure

ε_r : Dielectric constant of the substrate

λ: Free-space wavelength

c: Speed of light in free space

f_c :Center frequency

Phase response of reference microstrip line is given as

$$\emptyset_m = \beta_m \times l_m \tag{3.12}$$

$$\beta_m = 360° \times \frac{\sqrt{\varepsilon_e}}{\lambda} \tag{3.13}$$

$$\varepsilon_e = \frac{\varepsilon_r + 1}{2} + \frac{\varepsilon_r - 1}{2}\left(\sqrt{1 + \frac{12h}{W}}\right) \tag{3.14}$$

where

β_m : Effective phase constant of the microstripline

ε_e: Effective dielectric constant of the microstripline

l_m : Physical length of the microstripline

Hence differential phase shift of the whole structure is

$$\Delta\emptyset = \emptyset_c - \emptyset_m = 90° - 2\arctan\left[\frac{\tan(\beta_{ef} l)}{\sqrt{1 - C^2}}\right] - \beta_m \times l_m \tag{3.15}$$

Coupling coefficient of the structure is calculated selecting $\beta_{ef}l$=110° and l_m=2l for enlarged bandwidth [16]. This coupling value is used in the following equations in order to calculate the necessary dimensions.

Depending on the relationship between coupling value and even-odd mode impedance values, major diameters of the patch and slot can be calculated from the following equations.

$$Z_{oe} = \sqrt{\frac{1 + C}{1 - C}} = \frac{60\pi}{\sqrt{\varepsilon_r}} \frac{K(k_1)}{K'(k_1)} \tag{3.16}$$

$$Z_{oo} = \sqrt{\frac{1 - C}{1 + C}} = \frac{60\pi}{\sqrt{\varepsilon_r}} \frac{K'(k_2)}{K(k_2)} \tag{3.17}$$

where

K(k) : Elliptical integral of the first kind

and can be approximated by following equations

$$K'(k) = K(1-k^2) \tag{3.18}$$

$$\frac{K(k)}{K'(k)} = \begin{cases} \frac{2}{\pi}\ln\left(2\sqrt{\frac{1+k}{1-k}}\right), for\ 0.707 \le k \le 1 \\ 2\ln\left(2\sqrt{\frac{1+\sqrt{1-k^2}}{1-\sqrt{1-k^2}}}\right), for\ 0 \le k \le 0.707 \end{cases} \tag{3.19}$$

Finally, D_m and D_s can be extracted from the following equations

$$k_1 = \sqrt{\frac{sinh^2(\pi^2 D_s/(16h))}{sinh^2(\pi^2 D_s/(16h)) + cosh^2(\pi^2 D_m/(16h))}} \tag{3.20}$$

$$k_2 = tanh(\pi^2 D_m/(16h)) \tag{3.21}$$

Reference line length l_{ref} is approximated by

$$l_{ref} = l_m + 2l_t \tag{3.22}$$

and should be tuned for precise phase shift response.

Bandwidth of the structure mainly depends on keeping the coupling value constant over the design band. As well as the phase shift value and dimensions, phase deviation, return loss and insertion loss values are determined by this coefficient.

Considering the study in reference [16], it would not be futile to expect good return loss, insertion loss and relative phase error behaviors for phase shift values of $22.5° \le \Delta\varphi \le 45°$ over a coupling length of $36° \le \beta_{ef} l \le 144°$. This means that the structure is promising two-octave band operation. Due to the topology's wideband potential, a 2-6GHz phase shifter is intended to be designed while obeying other design criterion given in Table 3-1. 90°operation is provided by cascading two 45° degree sections. λ/4 transmission lines added at both ends of the difference path and in between the two sections increases the return loss bandwidth as quarter wavelength impedance transformation improves matching characteristics. Phase shift value of the structure is limited by the return loss for values except $22.5° \le \Delta\varphi \le 45°$ range, for two-octave operation.

Values of design parameters are calculated using Equations 3.9-3.21 as follows:

λ=75mm@4GHz, ε_r =3.66, ε_e ≈2.85, β_{ef} ≈ 9.2°/mm, β_m ≈ 8.1°/mm, l≈12mm, l_m≈24mm, C ≈ 0.73, D_m ≈ 4.8mm, D_s ≈ 7.5mm, lt=11mm and l_{ref}=95mm.

It is decided to use the mathematical dimensions in realization since the response could not be improved in optimization. The structure is constructed in HFSS™ as in Figure 3-15 with the obtained values of design parameters.

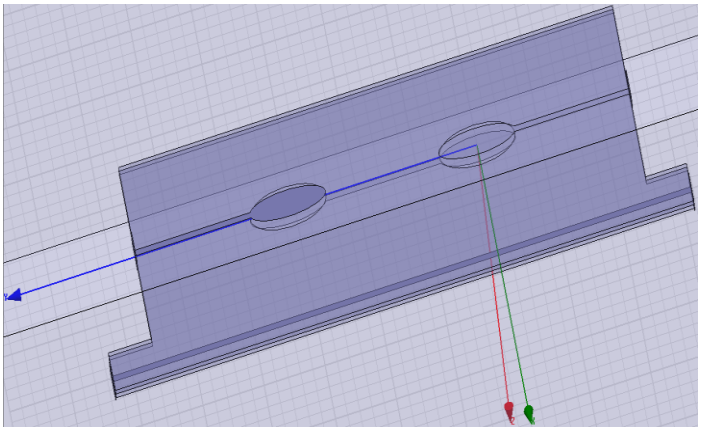

Figure 3-15 HFSS™ View of Designed Aperture Coupled Phase Shifter

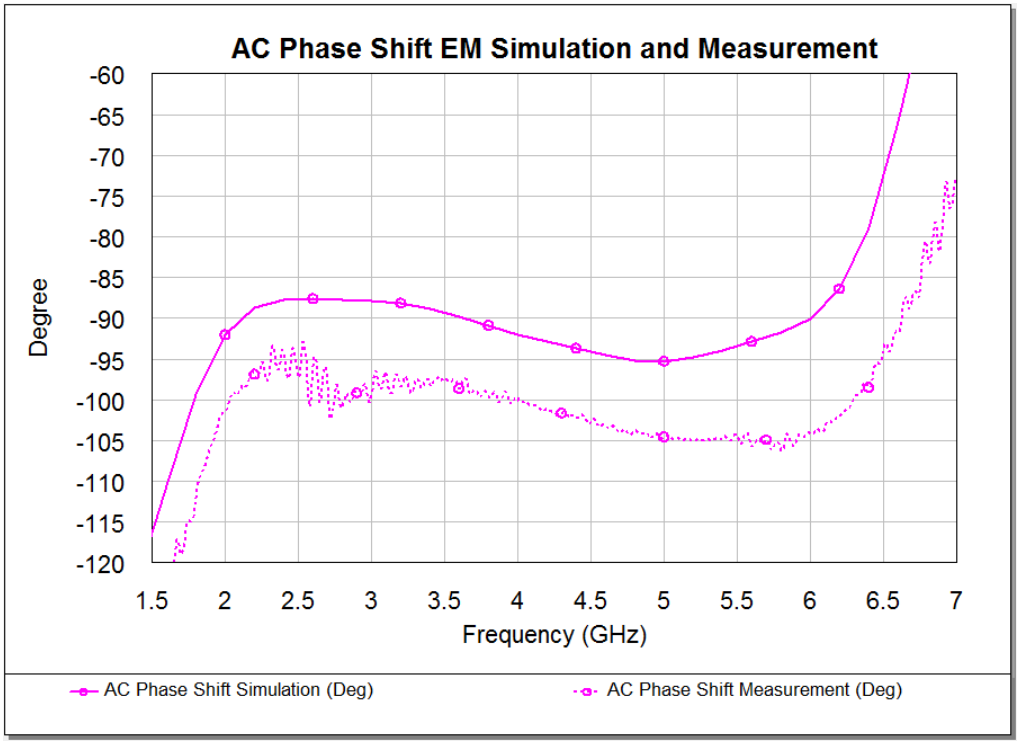

Figure 3-16 Aperture Coupler EM Simulation and Measurement of Phase Shift

Differential phase responses of simulated and fabricated circuits are given together in Figure 3-16. Simulation exhibits 90°±5° phase response between 1.9-6.25GHz whereas fabricated circuit has 100°±5° phase response between 1.9-6.5GHz. Around 10° difference between simulation and measurement results arises from, bad arrangement of coupling value and coupling length and mistuning of the reference transmission line.

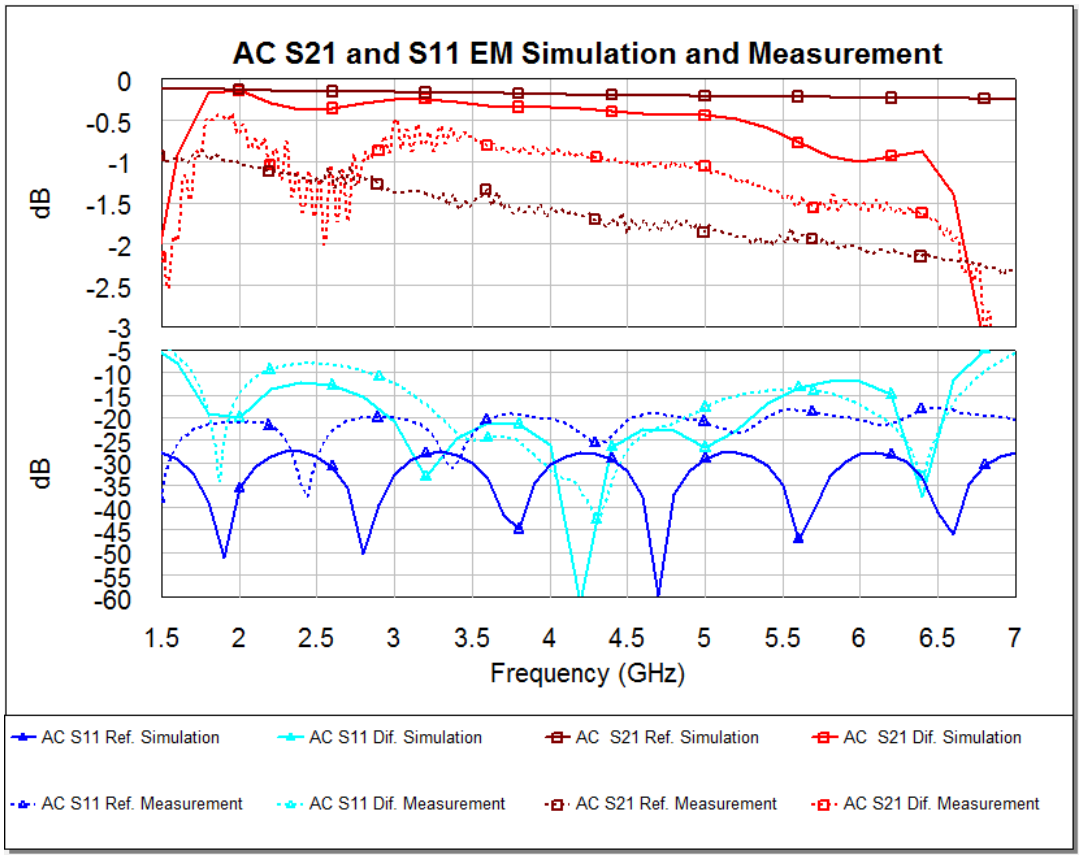

Figure 3-17 S_{21} and S_{11} Parameters of Designed and Fabricated Aperture Coupler Circuit

Amplitude responses of designed and fabricated circuit of reference and difference paths are given in Figure 3-17. Simulated circuit exhibits 12dB return loss at the worst point and 1.3±0.5dB insertion loss through 1.65-6.65GHz band whereas fabricated circuit has 8dB return loss in the worst point and 1.8±0.5dB insertion loss within the same band.

Difference between the insertion losses of the simulation and measurement results is caused by the connector losses. Insertion loss variation also increases by the addition of connectors as the loss of the connectors increase with frequency.

Corruption in amplitude and phase responses of the fabricated circuit between 2-3GHz can be explained by alteration of the coupling value across the band and using 110° coupling length instead of 90° [16]. This may be cured by optimizing coupling length value. However, there is a lesson to take. Amplitude imbalance is a source of phase imbalance; hence it should be kept as small as possible. Nonetheless, it is normal to have greater error in cascaded 90° structure than that of a single 45° structure.

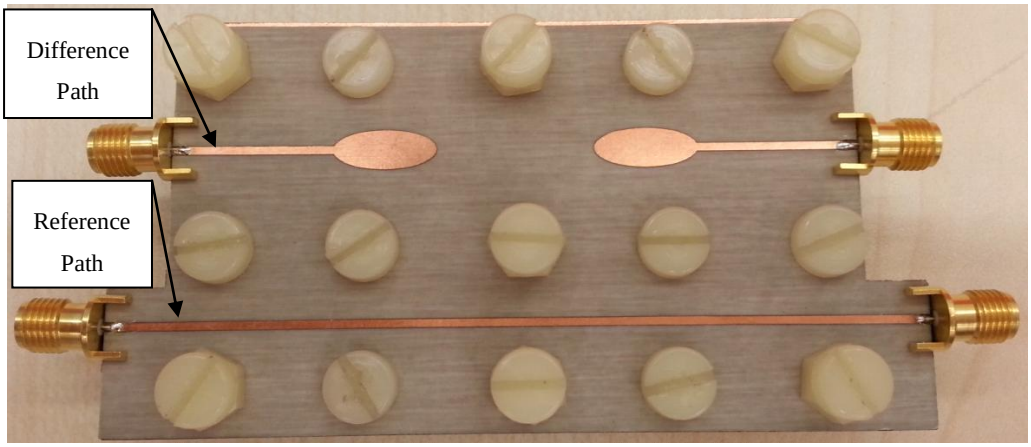

(a)

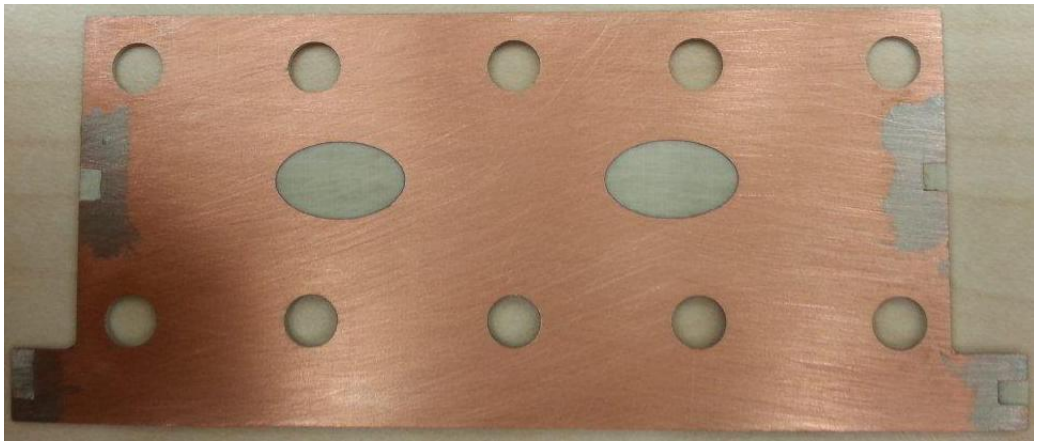

(b)

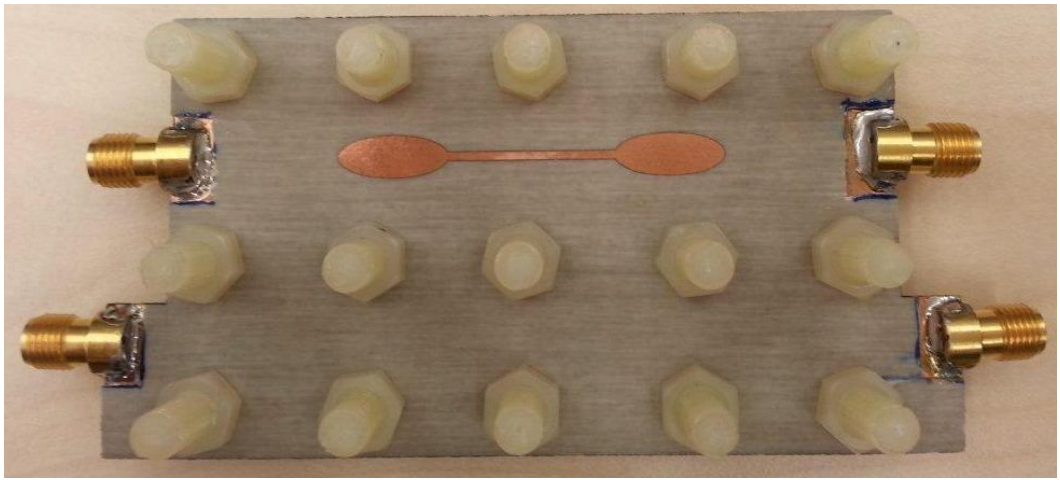

(c)

Figure 3-18 Fabricated Cascaded Aperture Coupler Based Phase Shifter Circuit
(a) Top Layer, (b) Mid-Layer, (c) Bottom Layer

Resultant structure occupies an area of 8cmx4cm. Nevertheless, size of the circuit can be reduced by bending rectangular transmission lines and using a substrate that has a higher dielectric constant. Although not employing lumped elements is a very important advantage for repeatability, the structure is more suitable for mass production when realized with modern multilayer production technologies e.g. LTCC [16]. However, patch-slot alignment when sticking two laminates together should be engineered carefully.

3.2.4 Double Shunt Stub Phase Shifter

Schematic view of double shunt stub phase shifter is given in Figure 3-19.

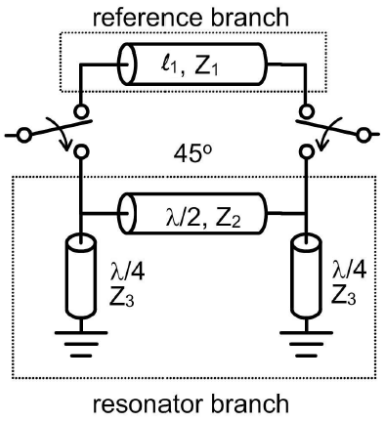

Figure 3-19 Schematic View of Double Shunt Stub Phase Shifter [46]

Mathematical expressions for calculation of dimensions of double shunt stub phase shifter demonstrated in Figure 3-19 are given below.

Perfect input match condition which implies S_{11}=0 yields following equation

$$Z_2^{'}\sin(\pi\omega^{'}) + \frac{\frac{Z_2^{'}\sin(\pi\omega^{'})}{Z_3^{'}\tan(0.5\pi\omega^{'})} + 2\cos(\pi\omega^{'})}{Z_3^{'}\tan(0.5\pi\omega^{'})} = \frac{\sin(\pi\omega^{'})}{Z_2^{'}} \tag{3.23}$$

Simplifying Equation 3.23 by setting $Z_2^{'} = 1$ and using the imformation that resonant frequencies are symmetrical around the normalized center frequency $\omega^{'} = 1$, $Z_3^{'}$ can be calculated by the following formula

$$\omega_{1,2}^{'} = 1 \pm \left(1 - \frac{2}{\pi}\tan^{-1}\sqrt{1 + \frac{1}{Z_3^{'2}}}\right) \tag{3.24}$$

Equations show that the phase slope can be controlled by adjusting $Z_2^{'}$ and $Z_3^{'}$ impedances. If the phase slope is arrenged to be equal to that of the reference transmission line, constant phase shift is achieved. With the decreasing phase shift value, stub widths reaches to practical limitations. In contrary, with the increasing phase shift value, return loss value gets unacceptably worse. Phase shift values between 20°-70° range are achievable with shunt stub topology [46]. Therefore, two 45° stages are cascaded to have 90° phase shift response. Shunt stubs are separated with a λ/2 transmission line in order to increase matching response by creating extra transmission poles.

For a 2-5 GHz phase shifter design, normalized impedance values are found as $Z_1^{'} = Z_2^{'} = 1$ and $Z_3^{'}$=2.4 using Equation 3.24. Line impedances are normalized according to 50Ω.

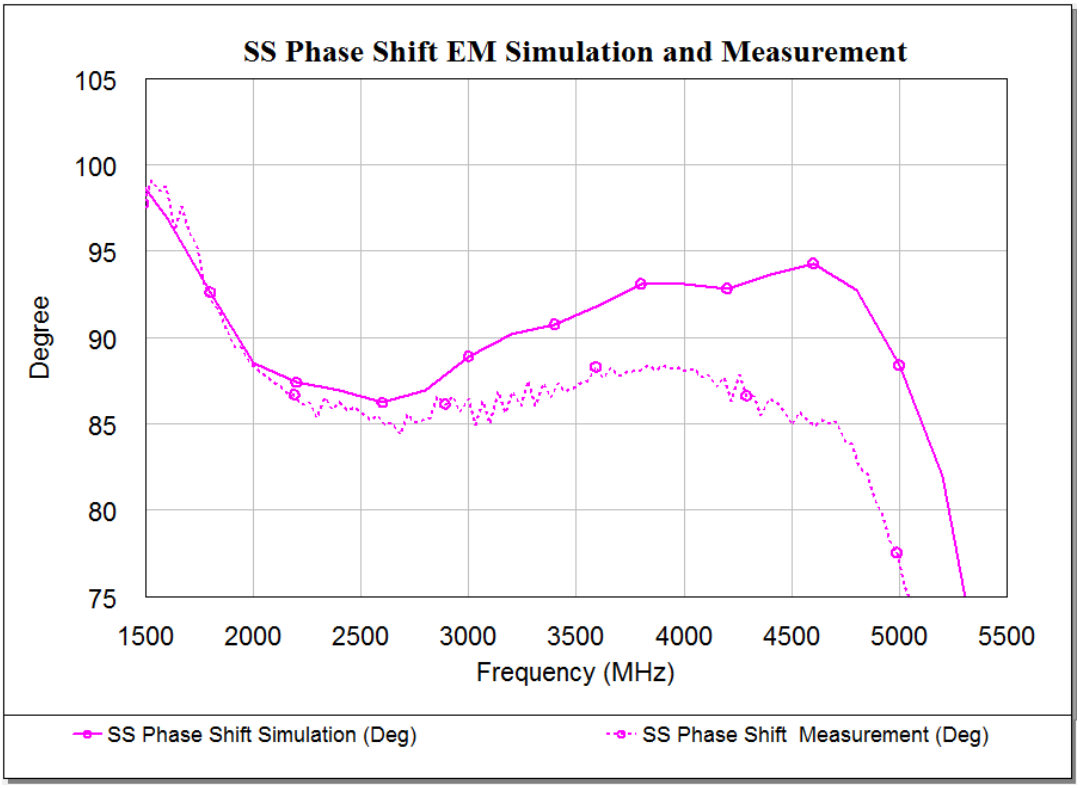

Figure 3-20 Shunt Stub EM Simulation and Measurement of Phase Shift

It is seen in Figure 3-20 that simulated circuit exhibits 90°±5° phase shift performance between 1700MHz and 5100MHz and fabricated circuit has 85°±5° phase shift response within 1900-4900MHz band. However S-band performance of the fabricated circuit is obviously better than simulation results.

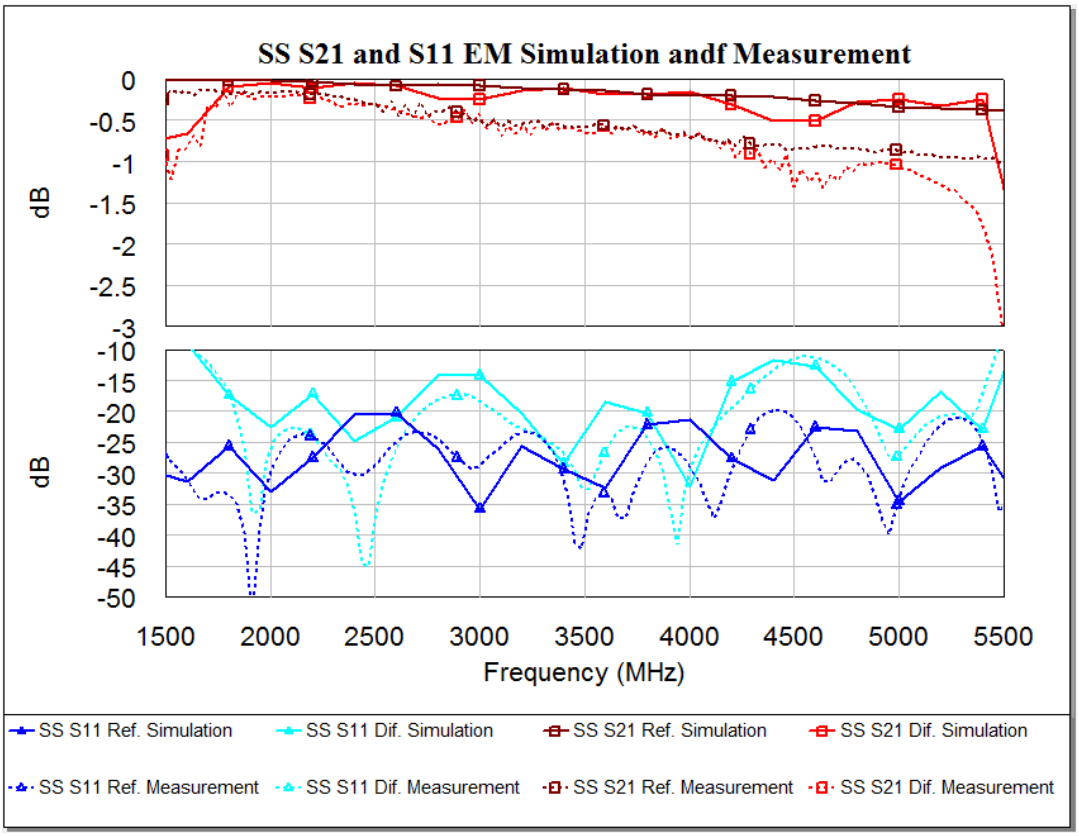

Figure 3-21 S_{21} and S_{11} Parameters of Designed and Fabricated Shunt Stub Circuit

Amplitude responses of reference and difference paths of designed and fabricated circuits are given in Figure 3-21. Insertion loss varies in the range of 0.25±0.25dB for the simulated and 1.1±0.9dB for the fabricated circuit for all states within 1600-5450MHz band .Return loss values of all states of both simulated and fabricated circuits are better than 10dB throughout the same band.

Well-grounding of shunt stubs is very important in shunt stub phase shifter design. Upper and lower faces should be connected with drill holes especially where shunt stubs meet the upper ground surface. Otherwise parasitic radiation reaches to ground over a longer path and that may create undesired effects in amplitude and phase responses.

Even though the structure does not claim for compactness, occupied area may be reduced by bending transmission lines and using a higher dielectric substrate. The power of the structure is in that it offers UWB performance on a single layer, without employing any coupled structure and lumped elements. This property ensures an easy fabrication and good repeatability.

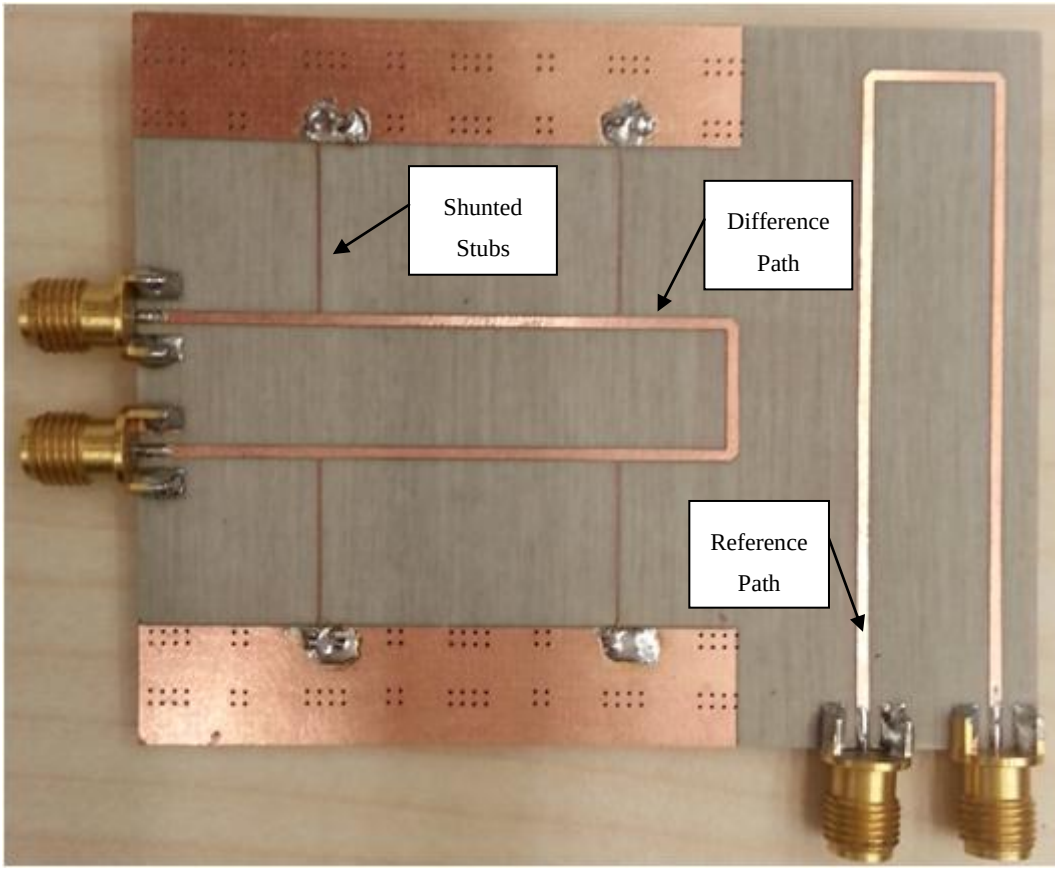

Figure 3-22 Fabricated Cascaded Double Shunt Stub Circuit

Dimensions of the final circuitry seen in Figure 3-22 is 7cmx6cm. Nevertheless, size of the circuit can be reduced by bending rectangular transmission lines and using a substrate that has a higher dielectric constant. Shunt stub phase shifter is suitable for mass production and PCB manufacturing technology due to consisting only of transmission lines employed on a single layer circuit. Theoretical and optimized values of dimensions for 2-5GHz design is given in Table 3-4. Dimension locations are mapped to Figure 3-19

Table 3-4 SS APF Theoretical and Optimized Values of TL Lengths

*All dimensions are in mils	w_1@50Ω	l1 tuned wrt l_2& l_3	w_2@50Ω	l_2@λ/2	w_3@120Ω	l_3@λ/4
Theoretical@ MATLAB	**43**	**1240**	**43**	**1000**	**5.8**	**530**
Optimized@EM	**40**	**1260**	**40**	**1000**	**6**	**560**

3.3 Comparison of Fabricated Phase Shifter Circuits

Among all design considerations topology and technology selection steps are very important as they affect probability of meeting design requirements. Many design requirements are determined by the application area. For example, for land based radar systems, weight and size may not be a big problem as in avionic radar systems meanwhile cost becomes more important in land based systems where a huge number of elements are employed. This brings designers to trade-off design decision between design criterion such as phase shift value, phase error, accuracy, loss, size and cost [45].

In short, different topologies may be convenient for different requirements and different applications; however they may be combined in same design to benefit from their powerful sides. For example, for an S-band 4-bit phase shifter design with 360° coverage, for 180° section, two-stage all pass filter based phase shifter topology for compactness; for 90° section, two cascaded 45° aperture coupled phase shifters for small phase error at a reasonable size, for 45° section, single shunt stub phase shifter for a low phase error and ease of manufacture, for 22.5° section, two-section loaded line phase shifter for ease of manufacture can be employed in same design. Cascading should be followed by a synthesis procedure in order to find the cascading order that gives the best electrical performance.

In PAR applications, as well as providing required electrical performance, a phase shifter must be compact (small and lightweight), easy to manufacture (simple and not requiring tuning) and massively producible (repeatable, maintainable, low cost).

Comparison of circuits according to S-Band performance and according to the phase error criteria are given in Table 3-5 and Table 3-6, respectively.

Table 3-5 Comparison of Electrical Performances of Investigated Circuits in S-Band

	Two-Stage All Pass Filter Phase Shifter	Eight-Section Loaded-Line Phase Shifter	Cascaded Aperture Coupler Phase Shifter	Cascaded Shunt Stub Phase Shifter
Phase Shift and Phase Error	**87°±2.5°@**	**95°±5°@**	**97°±5°@**	**86°±2°**
Amplitude Imbalance @Worst Data Point	**0.5dB**	**0.5dB**	**0.5dB**	**1dB**
Insertion Loss and Amplitude Variation @Worst Data Point	**1.1±0.5dB**	**1±0.7dB**	**1.3±0.7dB**	**1.1±0.9dB**
Return Loss @Worst Data Point	**<-10dB**	**<-10dB**	**<-8dB**	**<-17dB**

Table 3-6 Comparison of Fabricated Circuits According to Phase Error Criteria

	Two-Stage All Pass Filter Phase Shifter	Eight-Section Loaded-Line Phase Shifter	Cascaded Aperture Coupler Phase Shifter	Cascaded Shunt Stub Phase Shifter
Phase Shift and Phase Error	90°±5°@ 1.5-4.2GHz	95°±5°@ 2-4GHz	100°±5°@ 1.9-6.5GHz	85°±5°@ 1.9-4.9GHz
Amplitude Imbalance @Worst Data Point	0.5dB @2-4GHz	0.5dB @2-4GHz	0.5dB @1.65-6.65GHz	1dB 1.7-5.4GHz
Insertion Loss and Amplitude Variation @Worst Data Point	1.1±0.5dB @2-4GHz	1±0.7dB @2-4GHz	1.4±0.9dB @1.65-6.65GHz	1.1±0.9dB@ 1.7-5.4GHz
Return Loss @Worst Data Point	<-10dB @2-4GHz	<-10dB @2-4GHz	<-8dB @1.65-6.65GHz	<-10dB dB 1.7-5.4GHz
Size [cm x cm]	≈2x1	≈7x4	≈8x4	≈7x6
Cost in Multibit Design on account of Number of Switches	Low	Very High	High	High
Ease of Manufacture in PCB design	Moderate	Moderate	High	Very High
Suitability for Mass Production in PCB design	Low	Low	Moderate	High

CHAPTER 4

CONCLUSIONS

Phase shifters have many application areas, of which, study conducted in this thesis is concerned with their usage in phased array radars. They play a very important role in receivers and transmitters of support, attack and protection divisions of electronic warfare systems. In T/R modules of PAR systems, tunable phase shifters are indispensable elements of beam patterning together with tunable attenuators and amplifiers.

Modified versions of some phase shifter topologies are selected for design and production of S-Band 90° phase shifters with maximum of 10° peak-to-peak phase error and minimum of 10dB return loss at worst point. PCB production technology is chosen in accordance with the available laboratory facilities.

For each selected topology in this thesis, namely; two-stage all pass filter based phase shifter, eight-section loaded-line phase shifter, aperture coupler based phase shifter and double shunt stub phase shifter, following step-by-step fabrication procedure is applied. Firstly, theoretical background of the selected topology is given and the circuit is analyzed. Secondly, the circuit is designed, simulated and optimized in an appropriate design environment. Finally, the design is fabricated and measured. Simulation and measurement results are given in comparison for validation of the design. Additionally, experiments gained in design and production processes are shared. After that, fabricated designs are compared in some aspects, namely; electrical performance, size, cost, ease of manufacture, and suitability for mass production.

Ideally, an all pass filter passes all frequencies equally, however changing phase of the signal. In a single-stage all pass filter based phase shifter, difference between second order phase functions of reference and difference paths results in a second order phase shift function which has one point of inflection. This response is not sufficient for an octave band design. However, two-stage all pass filter is able to provide octave band response even when implied using COTS components. Element values of these components can be calculated by using p, q and Ω parameters which are related to the differential phase shift value of the critical points of the phase shift function.

In design, firstly, a MATLAB® code is developed for calculation of p, q and Ω parameters, after that, simulations are performed in AWR® design environment. In yield analysis, structure's dependence on lumped element tolerance values is revealed. This result shows that the structure has low repeatability. Moreover, in wideband (more than octave) or high frequency (more than 6GHz) or low phase shift bit (less than 11.25°) designs, necessity of very small value COTS components is an important drawback of the structure. Additionally, intermediate values which may not exist in the market may be required for implementation.

Intrinsically matched nature of all pass filters provides a good return loss characteristic. What is more, the structure is capable of providing up to 180° phase shift value in a single bit in a very compact form. Additionally, in a multibit design, same layout can be used for every phase shift bits. Simulation and measurement results are in good concordance. However, MIC technology is more suitable for production of this phase shifter as it offers higher repeatability and better ease of manufacture.

According to transmission line theory, loading a transmission line changes the phase characteristics of it. This property can be used for phase shifter design. In high phase shift bit (more than 11.25° for a conventional loaded line phase shifter) design, matching response of the circuit degrades drastically. Octave-band design is another problem. To handle these problems eight-section loaded-line circuit is designed. Every section providing around 11.25° at a good matching level makes 90° operation with a good matching characteristic possible.

In design, MATLAB® is utilized to calculate load susceptances. Then, simulations are run in AWR® design environment. Structure's dependence on lumped element tolerance values yields a limited repeatability. This may be healed by MIC realization of COTS components. Size of the circuit can be reduced by meandering lines and using higher dielectric substrates. Theoretically, quadrupling the dielectric constant of the circuit reduces transmission line lengths to their half. Eventually, it seems that it is better to use them for small phase shift bits as each section requiring a switching device is not cost effective. Implementation difficulty increases with number of sections.

In coupled structure based phase shifters, main problem is to keep coupling coefficient constant over the design band. Coupling coefficient determines phase shift, return loss, insertion loss and phase error values of the aperture coupler based phase shifter. As the phase shift value is determined together with return loss value by the coupling coefficient, a practical limitation to phase shift value emerges. HFSS™, 3D structural EM solver is used in design of the circuit. Because 45° is maximum achievable phase shift value of aperture coupler based phase shifter, two 45° degree sections are cascaded for 90° operation. Structure's main advantage is its potential to offer two-octave band operation. However in 2-6GHz design that is realized in this thesis, amplitude and phase performance of the circuit spoiled at the lower frequency edge. This may be healed by proper arrangement of the coupling coefficient, coupling length and reference microstrip line length. Nevertheless, it seems logical to use the structure for octave band operation which will probably permit excluding the part of the band where performance degrades and having lower phase error. In realization, patch slot alignment and high precision pattern sketching are very important as coupling coefficient is significantly affected by the geometry of the structure. Additionally, although nonexistence of COTS components yields high repeatability, it would have higher suitability for mass production when manufactured using modern multilayer production technologies that offer higher repeatability such as laminated multi-chip modules and LTCC.

In double shunt stub phase shifter, once the impedance of the half wavelength line of the resonator branch is set, phase shift, phase error, insertion loss and return loss values and bandwidth are determined by the impedance of the quarter wavelength shunt stubs. With the increasing shunt stub impedance, phase shift value decreases whereas return loss value increases, that is to say, every shunt stub impedance value has a definite phase shift and return loss value. Even though single shunt stub phase shifter could be sufficient, 45° sections are designed using double shunt stub topology for wider operational bandwidth with better return loss characteristics. After that, two identical 45° degree phase shifters are cascaded for 90° operation via a quarter wavelength transmission line to improve the return loss. Designed circuit is simulated in AWR® design environment. Fabricated circuit occupies a large area; however it can be reduced by meandering transmission lines and using a substrate that has higher dielectric constant. Nonexistence of COTS components and coupled lines and single layer production are advantageous properties for repeatability and mass production. Structure is very suitable for PCB technology and easy to design and manufacture.

Structures consisting only of transmission lines offer wider bandwidth than the ones employing COTS components (Hybrid structures). This is obviously because of the non-distributive nature of the COTS components. Hybrid structures also have lower repeatability because of the fact that COTS component tolerance values are far higher than the tolerance of pattern sketching process. What is more, hybrid structures are harder to manufacture due to the difficulties of soldering process. In coupled structures, constancy of the coupling value is hard to be maintained in realization. Production tolerances become excessively important. Uniformity of the laminate and precision of pattern sketching and layer alignment should be sufficient.

In future studies, all pass filter based phase shifter and loaded-line phase shifter can be realized in MIC design to get rid of performance dependence on COTS component tolerance values. Distributed realization of lumped elements permits higher repeatability, higher suitability for mass production, higher frequency and wider bandwidth design with better electrical performance and more precise phase shift adjustment in exchange for increased size. However, selecting high dielectric laminates can help on that. Coupling length adjustment can be investigated in order not to have performance degradation in some parts of the band. Additionally, requirement for quarter wavelength transmission lines should be investigated for size reduction. Double shunt stub phase shifter's electrical performance and size may be improved by utilizing PIN diodes where half-wavelength transmission line and shunt stubs intersect. This may cancel out the reference line and allow a better tuning over performance. Size may also be reduced by meandering lines and using laminates that have higher dielectric constants. Study can be extended by investigating more topologies realized on various substrates with various manufacturing technologies for numerous frequency bands. Experiences may be utilized for synthesizing a compact, low cost, easy to manufacture and massively producible phase shifter with good electrical characteristics.

REFERENCES

[1] S. Koul and B. Bhat, "Microwave and Millimeter Wave Phase Shifters," Volume I, Boston, MA: Artech House, 1991.

[2] Serraiocco, J., L., "Compact Phase Shifter Design Using Barium Strontium Titanate Thin Film Varactors," A master thesis submitted to the Department of Electrical and Computer Engineering of University of California at Santa Barbara, September 2003.

[3] A.G. Fox, "An Adjustable Waveguide Phase Changer," Proc. IRE, Vol. 35, pp. 1489-1498, December 1947.

[4] F. Reggia and E.G. Spencer, "A New Technique in Ferrite Phase Shifting for Beam Scanning of Microwave Antennas," Proc. IRE, Vol. 45, pp. 1510-1517, November 1957.

[5] B. Schiffman, "A New Class of Broadband Microwave 90-degree Phase Shifter," IRE Trans. Microwave. Theory Tech., Vol. MTT-6, No. 4, pp. 232-237, Apr. 1958.

[6] Ramos Quirarte, J.L. and J.P. Starski, "Synthesis of Schiffman Phase Shifters," IEEE Transactions on Microwave Theory and Techniques, Vol. 39, No. 11, pp. 1885-1889, November 1991.

[7] B. Schiek and J. Kohler, "A Method for Broad-Band Matching of Microstrip Differential Phase Shifters," IEEE Trans. Microwave. Theory Tech., vol. MTT-25, no. 8, pp. 666-671, Aug. 1977.

[8] V. P. Meschanov, I. V. Metelnikova, V. D. Tupkin, G. G. Chumaevskaya, "A New Structure of Microwave Ultra Wide Band Differential Phase Shifter," IEEE Transactions on Microwave Theory and Techniques, vol. 42, no. 5, May 1994.

[9] W. J. Brown and J. P. Starski, "A Broad-Band Differential Phase Shifter of Novel Design," in IEEE MTT-S Int. Microwave. Symp. Dig., vol. 3, pp. 1319-1322, 1999.

[10] Y. Guo, Z. Zhang, and L. Ong, "Improved Wideband Schiffman Phase Shifter," IEEE Trans. Microwave. Theory Tech., vol. 54, no. 3, pp. 1196-1200, Mar. 2006.

[11] S. Y. Eom, S. I. Jeon, J. S. Chae, and J. G. Yook, "Broadband 180º Bit Phase Shifter Using a New Switched Network," in IEEE MTT-S Int. Microwave. Symp. Dig., vol. 1, pp. 39-42, June 2003.

[12] Soon-Young Eom, "Broadband 180º Bit Phase Shifter Using λ / 2 Coupled Line and Parallel λ/ 8 Stubs," IEEE Microwave and Wireless Components Letters, vol. 14, no. 5, May 2004.

[13] S. Y. Zheng, S. H. Yeung, W. S. Chan, K. F. Man and S. H. Leung, "Improved Broadband Dumb-Bell-Shaped Phase Shifter Using Multi Section Stubs," Electronics Letters, vol. 44, no. 7, pp. 478-480, Mar. 2008.

[14] D. C. Boire, J. E. Dejenford, and M. Cohn, "A 4.5 to 18 GHz phase shifter," in IEEE MTT-S Int. Microwave Symp. Dig., 1985, pp. 601–604.

[15] Yong-Scheng Dai, Tang-Sheng Chen, "A Novel Ultra-Wideband 90° GaAs MMIC Phase Shifter with Either Analogue or Digital Control," Microwave Conference, 2000 Asia-Pacific IEEE pp. 1081-1084.

[16] Amin M. Abbosh, "Ultra-Wideband Phase Shifters," IEEE Trans. Microwave. Theory Tech., vol. 55, no. 9, pp. 1935-1941, Sep. 2007.

[17] Garver R., V., "Broad-Band Diode Phase Shifters," IEEE Transactions on Microwave Theory and Techniques, Vol. MTT-20, No. 5, pp. 314-323, May 1972.

[18] Guy D. Lynes, "Ultra Broadband Phase Shifters," Microwave Symposium Digest, G-MTT International, vol. 73, pp. 104-106, Jun 1973.

[19] J.F. White, "High Power, p-i-n Diode Controlled, Microwave Transmission Phase Shifters," IEEE Trans. Microwave Theory Tech., Vol. MTT-13, pp. 233-242, Mar.1965

[20] W. A. Little, J. Yuan, and C.C. Snellings, "Hybrid Integrated Circuit Digital Phase Shifters," in 1967 IEEE Int. Solid-State Circuits Conf. Dig., pp. 58-59.

[21] K. Hajek, J. Sedlacek and B. Sviezeny, "New Circuits for Realization of the 1st and 2nd Order All-Pass LC Filters with a Better Technological Feasibility," 2002 IEEE, vol. 3, pp. 523-526.

[22] K. Miyaguchi, M. Hieda, M. Hangai, T. Nishino, N. Yunoue, Y. Sasaki and M. Miyazaki, "An Ultra Compact C-Band 5 bit MMIC Phase Shifter Based on All-Pass Network," in Proceedings of the 1st European Microwave Integrated Circuits Conference, pp. 277-280, September 2006, Manchester UK.

[23] L.-Y. V. Chen, R. Forse, A. H. Cardona, T. C. Watson, R. York, "Compact Analog Phase Shifters using Thin-Film (Ba,Sr) TiO Varactors," Microwave Symp.3 2007, IEEE MTT-S, pp. 667-670, June 2007.

[24] D. Adler and R. Popovich, "Broadband Switched-Bit Phase Shifter Using All-Pass Networks," 1991 IEEE MTT-S Int. Microwave Symp. Dig., vol. 1, pp. 265-268, July 1991.

[25] G. M. Rebeiz, G. L. Tan, J. S. Hayden, "RF MEMS Phase Shifters: Design and Applications," IEEE Microwave Magazine, Vol. 3, pp. 72-81, June, 2002.

[26] Jung-Mu Kim, Sanghyo Lee, Jae-Hyoung Park, Chang-Wook Back, Youngwoo Kwon, and Yong-Kweon Kim, "A 5-17 GHz Wideband Reflection-Type Phase Shifter Using Digitally Operated Capacitive MEMS Switches," The 12th International Conference on Solid State Sensors, Actuators and Microsystems, pp. 907-910, Boston, June 8-12, 2003.

[27] Young J. KO, Jae Y. Park, and Jong U. Bu, "Integrated RF MEMS Phase Shifters with Constant Phase Shift," IEEE MTT-S International Microwave Symposium Digest, Vol. 3, pp. 1489-1492, 2003.

[28] S. Koul and B. Bhat, "Microwave and Millimeter Wave Phase Shifters," Volume II, Boston, MA: Artech House, 1991.

[29] D. C. Boire, G. St. Onge, C. Barratt, G. B. Norris, and A. Moysenko, "4: 1 bandwidth digital five-bit MMIC phase shifters," in IEEE Microwave and MM-Wave Monolithic Circuifs Symp., 1989, pp. 69-73.

[30] Hyukjin Kwon, Hongwook Lim, and Bongkoo Kang, "Design of 6-18 GHz Wideband Phase Shifters Using Radial Stubs," IEEE Microwave and Wireless Components Letters, Vol. 17, No. 3, pp. 205-207, March 2007.

[31] K. Miyaguchi, M. Hieda, K. Nakahara, H. Kurusu, M. Nii, M. Kasahara, T. Takagi, "An Ultra Broad Band Reflection Type 180º Phase Shifter with Series and Parallel LC Circuits," 2001 IEEE MTT-S Int. Microwave. Symp. Dig vol. 1, pp. 237-240.

[32] Mary Teshiba, Robert Van Leeuwen, Glenn Sakamoto, and Terry Cisco, "A SiGe MMIC 6-Bit PIN Diode Phase Shifter," IEEE Microwave and Wireless Components Letters, Vol. 12, No. 12, December 2002.

[33] Yong-Sheng Dai, Da-Gang Fang, and Yong-Xin Guo, "A Novel Miniature 1–22GHz 90 MMIC Phase Shifter with Microstrip Radial Stubs," IEEE Microwave and Wireless Components Letters, Vol. 18, No. 2, February 2008.

[34] L. Cheng-Jung, K.M.K.H. Leong, and T. Itoh, "Broadband quadrature hybrid design using metamaterial transmission line and its application in the broadband continuous phase shifter," IEEE MTT-S Int Microwave Symp (2007), pp. 1745–1748.

[35] Kholodnyak, D., Serebryakova, E., Vendik, I., Vendik, O., "Broadband digital phase shifter based on switchable right- and left-handed transmission line sections," IEEE Microwave and Wireless Components Letters, 16(5):258-260. 2006.

[36] Zou Yongzhuo; Hu Xin; Ling Ti; Lin Zhili; "New Differential Phase Shifter Using Novel Right-Handed Metamaterial Structures," Int. Sym. on Biophotonics, Nanophotonics and Metamaterials, 2006. Metamaterials 2006, pp. 536 – 538

[37] Y.Ayasli, S.Miller, R.Mozzi, L.Hanes, "Wide-Band Monolithic Phase Shifter," IEEE Transactions on Microwave Theory and Techniques, vol. MTT-32, no. 12, pp. 1710-1714, December 1984.

[38] Y. Ayasli et. al., "A Monolithic X-Band Four-Bit Phase Shifter," IEEE International Microwave Symp. , Vol. 82, Issue 1, pp. 486-488, 1982.

[39] D. Parker and D.C. Zimmerman, "Phased Arrays – Part II: Implementations, Applications, and Future Trends," IEEE Transactions on Microwave Theory Techniques, Vol.50, No.3, pp. 688–698, March 2002.

[40] I.D. Robertson and S. L1ucyszyn, "RFIC and MMIC Design and Technology," London, Institution of Electrical Engineers, 2001.

[41] Yaping Liang, C.W. Domier, and N.C. Luhmann,"MEMS Based True Time Delay Technology for Phased Antenna Array Systems," Asia-Pacific Microwave Conference, 2007.

[42] I.J. Bahl and P. Bhartia, “Microwave Solid State Circuit Design,” John Wiley and Sons, May 2003.

[43] Andricos, C., Bahl, I., J., Griffin, E., L., “C-Band 6-Bit GaAs Monolithic Phase Shifter”, Microwave and Millimeter-Wave Monolithic Circuits, Vol. 85, Issue 1, pp.8-9, June 1985.

[44] David M. Pozar, “Microwave Engineering,” John Wiley and Sons, 1998.

[45] Leo G. Maloratsky, “Integrated Microwave Front-Ends with Avionics Applications,” Artech House, 2012.

[46] X. Tang, K. Mouthaan, “Design of UWB Phase Shifter Using Shunt λ/4 Stubs,” IMS, 2009.

[47] Kaan Temir, “True-Time Delay Structures for Microwave Beamforming Networks in S-Band Phased Arrays,” A master thesis submitted to the Graduate School of Natural and Applied Sciences of Middle East Technical University, January 2013.

APPENDIX A

MATRIX REPRESENTATION OF MICROWAVE PHASE SHIFTERS

General matrix representation of non-reciprocal, lossy and frequency dependent phase shifter is given as

$$\begin{bmatrix} b_1 \\ b_2 \end{bmatrix} = \begin{bmatrix} |S_{11}(\omega)|\angle\gamma(\omega) & |S_{12}(\omega)|\angle\beta(\omega) \\ |S_{21}(\omega)|\angle\alpha(\omega) & |S_{22}(\omega)|\angle\delta(\omega) \end{bmatrix} \begin{bmatrix} a_1 \\ a_2 \end{bmatrix} \quad (\mathrm{A}.1)$$

Under perfect match condition which is

$$|S_{11}(\omega)| = |S_{22}(\omega)| = 0 \quad (A.2)$$

Matrix representation given in Equation A.1 simplifies to

$$\begin{bmatrix} b_1 \\ b_2 \end{bmatrix} = \begin{bmatrix} 0 & |S_{12}(\omega)|\angle\beta(\omega) \\ |S_{21}(\omega)|\angle\alpha(\omega) & 0 \end{bmatrix} \begin{bmatrix} a_1 \\ a_2 \end{bmatrix} \quad (A.3)$$

If the system is lossless

$$|S_{11}(\omega)|^2 + |S_{21}(\omega)|^2 = 1 \quad (A.4)$$

$$|S_{22}(\omega)|^2 + |S_{12}(\omega)|^2 = 1 \quad (A.5)$$

Solving Equations A.2, A.4 and A.5 simultaneously results in

$$|S_{21}(\omega)| = |S_{12}(\omega)| = 1 \quad (A.6)$$

For frequency independency

$$|S_{21}(\omega)|\angle\alpha(\omega) = |S_{21}|\angle\alpha \quad (A.7)$$

$$|S_{12}(\omega)|\angle\beta(\omega) = |S_{12}|\angle\beta \quad (A.8)$$

Using A.6, A.7 and A.8 gives following results

$$|S_{21}| = 1 \quad (A.9)$$

$$|S_{12}| = 1 \quad (A.10)$$

And matrix representation simplifies to

$$\begin{bmatrix} b_1 \\ b_2 \end{bmatrix} = \begin{bmatrix} 0 & \angle\beta \\ \angle\alpha & 0 \end{bmatrix} \begin{bmatrix} a_1 \\ a_2 \end{bmatrix} \quad (A.11)$$

A system is reciprocal if

$$[S] = [S]^T \tag{A.12}$$

Using Equation A.12 in A.11, following result is found

$$\begin{bmatrix} b_1 \\ b_2 \end{bmatrix} = \begin{bmatrix} 0 & \angle\alpha \\ \angle\alpha & 0 \end{bmatrix} \begin{bmatrix} a_1 \\ a_2 \end{bmatrix} \tag{A.13}$$

For a differential phase shifter, response of two states should be considered together. For a perfect match in this case, following condition must exist.

$$\left|S_{11}^{(1)}(\omega)\right| = \left|S_{22}^{(1)}(\omega)\right| = \left|S_{11}^{(2)}(\omega)\right| = \left|S_{22}^{(2)}(\omega)\right| = 0 \tag{A.14}$$

and a lossless system with perfect amplitude balance entails the following condition

$$\left|S_{21}^{(1)}(\omega)\right| = \left|S_{12}^{(1)}(\omega)\right| = \left|S_{21}^{(2)}(\omega)\right| = \left|S_{12}^{(2)}(\omega)\right| = 1 \tag{A.15}$$

Reciprocity implies following expressions

$$\left[S^{(1)}\right] = \left[S^{(1)}\right]^T \tag{A.16}$$

$$\left[S^{(2)}\right] = \left[S^{(2)}\right]^T \tag{A.17}$$

$$\alpha_2(\omega) - \alpha_1(\omega) = \beta_2(\omega) - \beta_1(\omega) \tag{A.18}$$

Frequency independency which implies that

$$\alpha_2(\omega) - \alpha_1(\omega) = \alpha_2 - \alpha_1 \tag{A.19}$$

Matrix representation of a lossless, reciprocal, frequency independent differential phase shifter is found as

$$\begin{bmatrix} b_1 \\ b_2 \end{bmatrix} = \begin{bmatrix} 0 & \angle(\alpha_2 - \alpha_1) \\ \angle(\alpha_2 - \alpha_1) & 0 \end{bmatrix} \begin{bmatrix} a_1 \\ a_2 \end{bmatrix} \tag{A.20}$$

APPENDIX B

DERIVATION OF ALL PASS FILTER PHASE CHARACTERISTICS

Appendix B is cited from reference [47].

General transfer function of any order APF is represented as

$$H(p) = \frac{D(-p)}{D(p)} \qquad (B.1)$$

where $p = \sigma + j\Omega$ and $D(p)$: Hurwitz Polynomial

The expression for a strict Hurwitz polynomial D(p) is

$$D(p) = \left(\prod_{k=1}^{n}[\rho - (-\sigma_k)]\right)\left(\prod_{i=1}^{m}[\rho - (-\sigma_i + j\Omega_i)]\,[\rho - (-\sigma_i - j\Omega_i)]\right) \qquad (B.2)$$

Where $(-\sigma_k)$: the left hand roots for $\sigma_k>0$ and $(-\sigma_i \pm j\Omega_i)$: complex left hand roots for $\sigma_i>0$ and $\Omega_i>0$.

For real frequencies, p=jΩ, amplitude response, |H(p)|, and phase response, $\phi_{H(j\Omega)}$ of any order APF are given as

$$|H(p)| = \sqrt{H(j\Omega) \times \overline{H(j\Omega)}} = \sqrt{\frac{D(-j\Omega)}{D(j\Omega)} \times \frac{D(j\Omega)}{D(-j\Omega)}} = 1 \qquad (B.3.a)$$

$$\phi_{H(j\Omega)} = -j\,ln\big(H(j\Omega)\big) \qquad (B.3.b)$$

If all poles and zeros of are placed only along the σ-axis, this type of network is called as C-type which forms 1st order APF networks. If the poles and zeros are all complex with quadrantal symmetry about the origin of the complex plane, this type of network is referred as D-type which generates 2nd order APF networks.

Y parameters for 2nd order APF are given as

$$Y_{11} = \frac{1 + s^2 C_1 L_1 \frac{1}{2(1+k)}}{sL\left(s^2 C_1 L_1 \frac{(1-k)}{4(1+k)} + 1\right)} + sC_2 \qquad (B.4.a)$$

$$Y_{21} = -\left[\frac{1 - s^2 C_1 L_1 \frac{k}{2(1+k)}}{sL\left(s^2 C_1 L_1 \frac{(1-k)}{4(1+k)} + 1\right)} + sC_2\right] \qquad (B.4.b)$$

$$Z_{in} = \sqrt{\left(\frac{L_1}{C_1}(1+k)\left(\frac{1+s^2C_1\frac{L_1}{2}(1-k)}{1+2s^2C_2L_1(1+k)}\right)\right)} \qquad (B.4.c)$$

The condition for Z_{in} to become a pure, real and frequency invariant impedance is

$$C_2 = C_1\frac{1-k}{4(1+k)} = \alpha C \qquad (B.4.d)$$

If Z_{in} is equal to the characteristic impedance Z_0, then the relation between the elements used in modified t-section circuit is

$$\frac{L_1}{C_1} = \frac{{Z_0}^2}{2(1+k)} \qquad (B.4.e)$$

Converting Y-parameters to S-Parameters yields

$$S_{21} = \frac{-2Y_{21}\sqrt{R_{01}R_{02}}}{(1+Y_{11}Z_{01})(1+Y_{22}Z_{02}) - Y_{21}Y_{12}Z_{01}Z_{02}} \qquad (B.5)$$

where $Y_{11} = Y_{22}$ and $Y_{21} = Y_{12}$ for symmetric network

Substituting the equations (B.4.a)-(B.4.e) into the equation (B.5) gives the transfer function of the circuit as

$$H(jw) = \frac{\left(\frac{f}{f_0}\right)^4\alpha(k-1) - \left(\frac{f}{f_0}\right)^2\left(2k - 4\alpha(k+1)\right) - 4(k+1)}{\left[-\left(\frac{f}{f_0}\right)^2\alpha + \left(\frac{f}{f_0}\right)\frac{j}{2} + 1\right]\left[\left(\frac{f}{f_0}\right)^2(1-k) - j\left(\frac{f}{f_0}\right)(k+1) - 4(k+1)\right]} \qquad (B.6)$$

Transfer function of a 2nd order APF derived from the equation (B.1) and (B.2) is

$$H(s) = \frac{s^2 - s\left(\frac{\omega_0}{Q}\right) + (\omega_0)^2}{s^2 + s\left(\frac{\omega_0}{Q}\right) + (\omega_0)^2} \qquad (B.7)$$

If the equations (B.6) and (B.7) are compared, then the relation between Q and k is obtained as

$$Q = \sqrt{\frac{1-k}{1+k}} \qquad (B.8)$$

APPENDIX C

MATLAB® CODE FOR CALCULATION OF p, q AND Ω PARAMETERS OF ALL PASS FILTER

```
%Two Stage ALLPASS Filter_Phase_Shifter
clear;
clc;
close all;
F_min=input('Insert min Frequency in GHz  ');
F_max=input('Insert max Frequency in GHz  ');
B=F_max/F_min;%Bandwidth of the phase shifter
Zo=input('Insert I/O Impedance value wrt Ohm  ');
Ch=input('For 1 bit SP2T solution enter "0"; for 2 Bit SP4T solution enter "(1)"   ');
phi_delta=input('Insert Required Phase Shift in Degree; Ex: [-22.5 -45   ...]   ');
wm=2*pi*sqrt(F_max*F_min)*1e9; % centered frequency
p_s=1.0:0.001:1.5; %Define freq ratio upper/lower
q_s=1.0:0.001:1.6; %Define freq ratio upper/lower
phi_B=zeros(length(p_s),length(q_s)); %Phase Value @ the end of Band
phi_min=phi_B; %Min Phase Value inside the Band
phi_1=phi_B; %Phase Value @ the beginning of Band
OUTPUT_ALL=zeros(length(phi_delta),12);
omega=1.0/sqrt(B):0.01:sqrt(B); %Normalized Freq Band

for n=1:length(phi_delta);
   phi_m=phi_delta(n);

   %Calculating Phase Error by using Delta_phi Function
   for jk=1:length(p_s)
      for jl=1:length(q_s)
      phi_B(jk,jl)=delta_phi(p_s(jk),q_s(jl),sqrt(B));
      phi_1(jk,jl)=delta_phi(p_s(jk),q_s(jl),1.0);
      phi_min(jk,jl)=min(delta_phi(p_s(jk),q_s(jl),omega));
      end
   end

   %Calculating Cost Analysis to obtain Best "p" and "q" values.
   w=0.90;
   dphi_des=9.0;
cost=w*abs(phi_m*ones(length(p_s),length(q_s))-0.5*(phi_B+phi_min)).^2.0+(1-
w)*(abs(0.5*(phi_B-phi_min))/phi_m).^2+(abs(0.5*(phi_B-
phi_min))>=dphi_des)*1e16+(phi_1>phi_B)*1e16;
 [ind1,ind2]=find(cost==min(min(cost)));%Obtaining index number for "p" and "q"
```

```
%Deriving "p" and "q" values
   p_fin=p_s(ind1);q_fin=q_s(ind2);
      %Inductance values are in terms of nH and capacitance values are in terms of pF
      L1=p_fin*q_fin*Zo/wm*1e9;
      L2=(p_fin*Zo)/(q_fin*wm)*1e9;
      L3=Zo/(p_fin*q_fin*wm)*1e9;
      L4=(q_fin*Zo)/(p_fin*wm)*1e9;
      C1_1=(p_fin*q_fin)/(2*Zo*wm)*1e12;
      C1_2=(2*p_fin*q_fin)/(Zo*wm)*1e12;
      C2_1=(p_fin/(2*q_fin*Zo*wm))*1e12;
      C2_2=(2*p_fin/(q_fin*Zo*wm))*1e12;
      C3_1=1/(2*p_fin*q_fin*Zo*wm)*1e12;
      C3_2=2/(p_fin*q_fin*Zo*wm)*1e12;
      C4_1=(q_fin/(2*p_fin*Zo*wm))*1e12;
      C4_2=(2*q_fin/(p_fin*Zo*wm))*1e12;

OUTPUT_ALL(n,:)=[C1_1,C1_2,C2_1,C2_2,C3_1,C3_2,C4_1,C4_2,L1,L2,L3,L4]
end

% Delta_phi Function
function out=delta_phi(p,q,omega)
out=2.0*180.0/pi*(atan(omega/p/q-p*q./omega)-atan(omega*p/q-
q./omega/p)+atan(omega*q/p-p./omega/q)-atan(omega*p*q-1.0./omega/p/q));
end
```